

# NAVAL POSTGRADUATE SCHOOL MONTEREY, CALIFORNIA



## THESIS

### RADAR CROSS SECTION SYNTHESIS OF DOUBLY CURVED SURFACES

by

Rachel C. Waddell

September, 1995

Thesis Advisor:

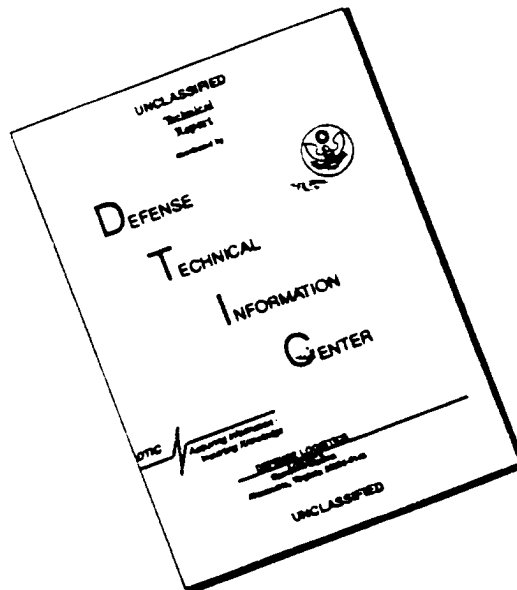
David C. Jenn

Approved for public release; distribution is unlimited.

DTIC QUALITY INSPECTED 1

19960319 103

# DISCLAIMER NOTICE



THIS DOCUMENT IS BEST QUALITY AVAILABLE. THE COPY FURNISHED TO DTIC CONTAINED A SIGNIFICANT NUMBER OF PAGES WHICH DO NOT REPRODUCE LEGIBLY.

REPORT DOCUMENTATION PAGE			Form Approved OMB No. 0704-0188	
Public reporting burden for this collection of information is estimated to average 1 hour per response, including the time for reviewing instruction, searching existing data sources, gathering and maintaining the data needed, and completing and reviewing the collection of information. Send comments regarding this burden estimate or any other aspect of this collection of information, including suggestions for reducing this burden, to Washington Headquarters Services, Directorate for Information Operations and Reports, 1215 Jefferson Davis Highway, Suite 1204, Arlington, VA 22202-4302, and to the Office of Management and Budget, Paperwork Reduction Project (0704-0188) Washington DC 20503.				
1. AGENCY USE ONLY (Leave blank)		2. REPORT DATE September 1995		3. REPORT TYPE AND DATES COVERED Master's Thesis
4. TITLE AND SUBTITLE RADAR CROSS SECTION SYNTHESIS OF DOUBLY CURVED SURFACES			5. FUNDING NUMBERS	
6. AUTHOR(S) Waddell, Rachel C.				
7. PERFORMING ORGANIZATION NAME(S) AND ADDRESS(ES) Naval Postgraduate School Monterey CA 93943-5000			8. PERFORMING ORGANIZATION REPORT NUMBER	
9. SPONSORING/MONITORING AGENCY NAME(S) AND ADDRESS(ES)			10. SPONSORING/MONITORING AGENCY REPORT NUMBER	
11. SUPPLEMENTARY NOTES The views expressed in this thesis are those of the author and do not reflect the official policy or position of the Department of Defense or the U.S. Government.				
12a. DISTRIBUTION/AVAILABILITY STATEMENT Approved for public release; distribution is unlimited.			12b. DISTRIBUTION CODE	
13. ABSTRACT (maximum 200 words) The radar cross section (RCS) of various geometries with surface resistivity is synthesized using a physical optics approximation. Using the RCS, a set of equations are developed for reconstructing the resistivity across the surface. The reconstructed resistivity is then compared with the original resistivity and the RCS recalculated using the synthesized resistivity to validate the accuracy of the synthesis procedure.				
14. SUBJECT TERMS Radar Cross Section, Physical Optics Approximation, Surface Resistivity			15. NUMBER OF PAGES 120	
			16. PRICE CODE	
17. SECURITY CLASSIFICATION OF REPORT Unclassified	18. SECURITY CLASSIFICATION OF THIS PAGE Unclassified	19. SECURITY CLASSIFICATION OF ABSTRACT Unclassified	20. LIMITATION OF ABSTRACT UL	



Approved for public release; distribution is unlimited.

**RADAR CROSS SECTION SYNTHESIS  
OF  
DOUBLY CURVED SURFACES**

Rachel C. Waddell  
GS-12/3, United States Air Force  
B.S.E.E., Florida State University , 1990

Submitted in partial fulfillment  
of the requirements for the degree of

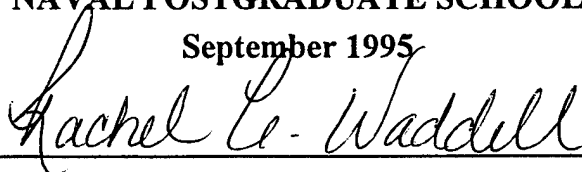
**MASTER OF SCIENCE IN ELECTRICAL ENGINEERING**

from the

**NAVAL POSTGRADUATE SCHOOL**

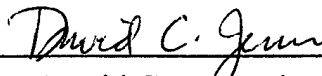
September 1995

Author:

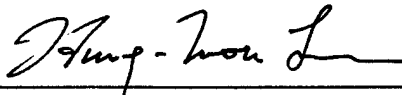


Rachel C. Waddell

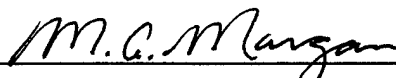
Approved by:



David C. Jenn, Thesis Advisor



Hung-Mou Lee, Second Reader



Michael A. Morgan, Chairman

Department of Electrical and Computer Engineering



## ABSTRACT

The radar cross section (RCS) of various geometries with surface resistivity is synthesized using a physical optics approximation. Using the RCS, a set of equations are developed for reconstructing the resistivity across the surface. The reconstructed resistivity is then compared with the original resistivity and the RCS recalculated using the synthesized resistivity to validate the accuracy of the synthesis procedure.



## TABLE OF CONTENTS

I. INTRODUCTION . . . . .	1
II. THEORETICAL BACKGROUND . . . . .	5
A. RCS FROM THE SCATTERED FIELD . . . . .	5
B. SURFACE IMPEDANCES . . . . .	7
C. REFLECTION AND TRANSMISSION COEFFICIENTS . . . . .	9
1. TM Polarization . . . . .	9
2. TE Polarization . . . . .	10
D. PHYSICAL OPTICS APPROXIMATION . . . . .	11
III. FORMULATION AND SOLUTION . . . . .	13
A. BISTATIC CASE . . . . .	16
1. Flat Disk . . . . .	16
a. TM Polarization . . . . .	17
b. TE Polarization . . . . .	24
c. Arbitrary Polarization . . . . .	26
2. Doubly Curved Surfaces . . . . .	28
B. MONOSTATIC CASE . . . . .	30
C. SYNTHESIS EQUATIONS . . . . .	31
IV. COMPUTER IMPLEMENTATION AND DATA ANALYSIS . . . . .	37
A. RCS FROM THE SCATTERED FIELD . . . . .	37
B. RCS SYNTHESIS . . . . .	49
V. CONCLUSIONS . . . . .	67
APPENDIX. COMPUTER CODES . . . . .	69
LIST OF REFERENCES . . . . .	109
INITIAL DISTRIBUTION LIST . . . . .	111

## I. INTRODUCTION

During the middle 1950's, the idea of making platforms unobservable or less observable to radar was initiated by Bill Bahret of Wright Air Development Center. [Ref. 1] The initial motivation for low-observability came from the need to increase screening provided by a jammer. [Ref. 1] Subsequently, a great deal of research in the area of radar cross section (RCS) began.

There are four common methods for reducing the RCS of a given platform. They are [Ref. 2]:

1. shaping,
2. surface material selection,
3. active cancellation, and
4. passive cancellation.

Shaping to reduce RCS requires reducing the surface area that is perpendicular to the radar source. Surface material selection requires the addition of lossy materials to the surface of the target. Active cancellation is a method of reproducing the signal  $180^\circ$  out of phase from the radar. Passive cancellation is the addition of a secondary scatterer to cancel the reflected field from the primary target.

In this thesis, a synthesis method that can be used for surface material selection is addressed. That is, given the monostatic RCS of a platform, a set of equations are presented which can be used to choose the required material. Selecting a surface material that reduces the RCS of a platform requires the use of a radar absorbing material (RAM). Other types of

materials used in the reduction of RCS include resistive and conductive films, described in terms of ohms per square ( $\Omega/\square$ ) or mhos per square ( $\text{U}/\square$ ), respectively.

Metal surfaces such as those used for aircraft and ships closely approximate a perfect electric conductor (PEC). The addition of RAM to a surface causes it to have an inductive or capacitive surface impedance rather than that of a PEC. Impedance surfaces can absorb radar frequency (RF) energy thereby causing a reduction in the scattered energy.

An impedance surface supports both equivalent magnetic and electric currents. However, there are two special cases of impedance surfaces that only support either equivalent magnetic or electric currents: a resistive surface does not support equivalent magnetic currents, and a conductive sheet does not support electric currents. The resistive surface is the focus of this thesis, because its use greatly simplifies the equations used in the synthesis procedure.

A synthesis procedure can be developed based on the desired RCS for a particular target. The surface is separated into triangular subsections, or patches. The surface impedance across each subsection is assumed to be constant but can vary from patch to patch. A matrix equation is derived consisting of a vector of the known scattered field, a target surface scattering matrix, and a surface impedance vector. By solving the matrix equation, the impedance vector is obtained and the material properties of the surface can be determined.

In Chapter II, the theoretical background required to evaluate the RCS of a surface is presented. Surface impedances, reflection and transmission coefficients and the

physical optics approximation are examined.

In Chapter III, the synthesis procedure is developed. The procedure is applied to doubly curved surfaces such as spheres or portions of spheres.

In Chapter IV, the results of the synthesis procedure are compared to the exact solution. Finally, in Chapter V, an analysis of the results is given as well as recommendations for future work in this area.



## II. THEORETICAL BACKGROUND

In this chapter, the basic equations of electromagnetic scattering are presented.

### A. RCS FROM THE SCATTERED FIELD

The RCS of a target can be determined once its scattered field is known [Ref. 3]

$$\sigma = \lim_{r \rightarrow \infty} \left( \frac{4\pi r^2 |\bar{E}_s|^2}{|\bar{E}_i|^2} \right). \quad (2.1)$$

The scattered field arises from the currents induced by the plane wave on the target surface. The scattered electric field far from the target is given in terms of the electric ( $\bar{J}$ ) and equivalent magnetic ( $\bar{M}$ ) currents by [Ref. 4]

$$E_\theta = -j \frac{ke^{-jkr}}{4\pi r} (L_\phi + \eta N_\theta), \quad (2.2)$$

$$E_\phi = j \frac{ke^{-jkr}}{4\pi r} (L_\theta - \eta N_\phi), \quad (2.3)$$

where:

$$N_\theta = \iint_s (J_x \cos\theta \cos\phi + J_y \cos\theta \sin\phi - J_z \sin\theta) e^{jkr' \cos\psi} ds', \quad (2.4)$$

$$N_\phi = \iint_s (-J_x \sin\phi + J_y \cos\phi) e^{jkr' \cos\psi} ds', \quad (2.5)$$

$$L_{\theta} = \iint_{\Sigma} (M_x \cos \theta \cos \phi + M_y \cos \theta \sin \phi - M_z \sin \theta) e^{jkr' \cos \psi} ds' , \quad (2.6)$$

$$L_{\phi} = \iint_{\Sigma} (-M_x \sin \phi + M_y \cos \phi) e^{jkr' \cos \psi} ds' . \quad (2.7)$$

In equations (2.2) through (2.7)  $k$  is the wave number ( $2\pi/\lambda$ ,  $\lambda$  being the wavelength). The geometry is shown in Figure 1 below. The angles  $\theta$  and  $\phi$  are the standard spherical angles. For the remainder of this thesis, only resistive sheets are considered and therefore,  $M_x = M_y = M_z = 0$ .

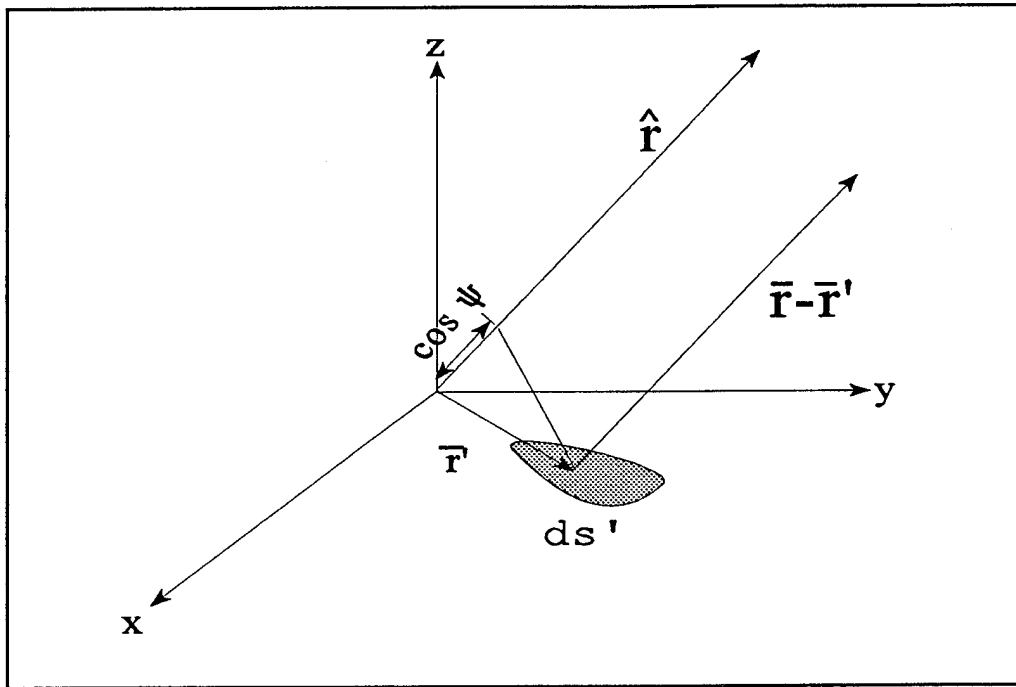


Figure 1. Coordinate system.

## B. SURFACE IMPEDANCES

Traditionally, most aircraft and ships were made of materials which are considered to be perfect conductors. Conducting targets generally have a high RCS relative to those of other materials. In RCS reduction (RCSR), the selection of materials for a target can reduce the scattered field. One method is to coat a perfectly conducting target with RAM. This yields a heavy target and is not an effective way to reduce RCS. Another approach is to use composite materials with some loss introduced. The latter approach is more efficient, since composites are frequently used in the manufacture of aircraft and ships. Composites can be characterized by their complex index of refraction,  $n_r$ , which is related to the permittivity and permeability of the material

$$n_r = \sqrt{\epsilon_s \mu_s} \quad (2.8)$$

where  $\epsilon_s$  is the permittivity of the material and  $\mu_s$  is the permeability of the material. The permittivity and permeability are usually complex numbers and it is the imaginary parts which contribute to losses. [Ref. 2] Thin layers of lossy material can be applied to a dielectric to cause the surface to be resistive and, no magnetic currents will flow on the surface.

If the target consists of composite materials then there is some penetration of the field into the target. The integrals in equations (2.4) and (2.5) become volume integrals because the currents exist below the surface. This is very

inconvenient computationally, and the problem can be avoided using the surface impedance approximation, also known as the Leontovich boundary condition

$$\eta_s = \frac{\bar{E}_{\tan}}{\bar{H}_{\tan}} . \quad (2.9)$$

$\bar{E}_{\tan}$  and  $\bar{H}_{\tan}$  are the total tangential fields on the outer surface of the target and  $\eta_s$  is its surface impedance in ohms ( $\eta_s=0$  if the surface is a PEC). [Ref. 3] Thus the original target surface can be replaced by a surface with impedance  $\eta_s$  and the same scattered fields result. Note that  $\eta_s$  depends on the location on the surface and the incidence direction.

Using equation (2.9), a set of vector equations can be derived

$$\bar{E} - \hat{n} (\hat{n} \cdot \bar{E}) = \eta_s \bar{J}_s , \quad (2.10)$$

$$\bar{H} - \hat{n} (\hat{n} \cdot \bar{H}) = \frac{\bar{M}_s}{\eta_s} . \quad (2.11)$$

For a resistive surface, this simplifies to

$$\hat{n} \times (\hat{n} \times \bar{E}) = -R_s \bar{J}_s , \quad (2.12)$$

$$\hat{n} \times (\hat{n} \times \bar{H}) = 0 , \quad (2.13)$$

where  $R_s$  is the resistivity of the material.

### C. REFLECTION AND TRANSMISSION COEFFICIENTS

The reflection coefficients quantify the amount of reflection and transmission of an electromagnetic wave that occurs at an interface between two different impedances. For a PEC, the incident wave is totally reflected, yielding a reflection coefficient of -1. The reflection ( $\Gamma$ ), absorption ( $A$ ), and transmission ( $T$ ) coefficients must obey the conservation of energy as shown below [Ref. 2]:

$$|\Gamma|^2 + |A|^2 + |T|^2 = 1. \quad (2.14)$$

For a lossless material,  $A=0$ .

The transmission and reflection coefficients are easily derived with the assumption that the surface is locally flat. Two principle polarizations must be considered: 1) transverse magnetic to the  $z$  axis (TM) and 2) transverse electric to the  $z$  axis (TE). An arbitrary polarized wave can be handled as a combination of the two principal polarizations.

#### 1. TM Polarization

For TM polarization, the incident wave is

$$\vec{E}_i = \hat{\theta} E_0 e^{-j\vec{k}_i \cdot \vec{r}} \quad (2.15)$$

where  $\vec{k}_i$  is the incident wave vector. For a TM polarized incident wave, the reflection coefficient for a resistive film is [Ref. 5]

$$\Gamma_{TM} = \frac{-\eta_o \cos \theta_i}{2R_s + \eta_o \cos \theta_i} \quad (2.16)$$

where  $\theta_i$  is the angle of incidence with respect to the z axis. If no absorption occurs, as is the case with an infinitely thin sheet, the transmission coefficient is

$$T_{TM} = \frac{2R_s}{2R_s + \eta_o \cos \theta_i} \quad (2.17)$$

The scattered field then becomes

$$\bar{E}_s = \theta \Gamma_{TM} E_o^i e^{-j\bar{k} \cdot \bar{r}} \quad (2.18)$$

where  $\bar{k}$  is the wave vector in the direction of observation.

## 2. TE Polarization

For TE polarization, the incident wave is

$$\bar{E}_i = \phi E_o^i e^{-j\bar{k}_i \cdot \bar{r}} \quad (2.19)$$

For a TE polarized incident wave, the reflection coefficient is [Ref. 5]

$$\Gamma_{TE} = \frac{-\eta_o}{2R_s \cos \theta_i + \eta_o} \quad (2.20)$$

With no absorption, the transmission coefficient is given by

$$T_{TE} = \frac{2R_s \cos \theta_i}{2R_s \cos \theta_i + \eta_0} \quad (2.21)$$

and the scattered field becomes

$$\bar{E}_s = \hat{\phi} \Gamma_{TE} E_\phi^i e^{-j\bar{k} \cdot \bar{r}}. \quad (2.22)$$

#### D. PHYSICAL OPTICS APPROXIMATION

The field incident on an illuminated object causes currents to flow on its surface. To solve exactly for the scattered electric field, these currents must be known. It is a lengthy and complicated process to solve for the currents. However, the incident field and the boundary conditions are known. Therefore an approximation can be made using the known incident field. The standard physical optics approximation is given by [Ref. 3]:

$$\bar{J}_s = 2 \hat{n} \times \bar{H}_i. \quad (2.23)$$

Equation (2.23) holds for the portion of the object which is illuminated. Physical optics approximation assumes the current along the surface drops to zero on areas of the object which are shaded from the illuminated field. In actuality, currents do not drop abruptly to zero. The currents slowly decay towards zero, but for electrically large bodies the error is negligible.

The physical optics approximation does not account for waves traveling along the surface of the object. Therefore, there is a decrease in RCS as the incident angle moves towards surface grazing and the sidelobes of the RCS pattern are lower than the actual values. The specular lobe level of the RCS pattern for flat or gently curved surfaces is generally within a few percent of the actual value.

### III. FORMULATION AND SOLUTION

The analysis of scattering from an arbitrary finite doubly curved surface requires the use of triangular subsections. The physical optics approximation and boundary conditions are used to obtain the synthesis equations. The synthesis equations are then verified by comparing with calculated fields. The geometries considered for this calculation are a flat disk and a spherical cap. The geometries are shown in Figures 2 and 3.

The incident wave is assumed to be a planar wave with arbitrary polarization. Both TM and TE components exist. The incident field is given by

$$\bar{E}_i = (\hat{\theta} E_\theta^i + \hat{\phi} E_\phi^i) e^{-j\bar{k}_i \cdot \bar{r}}, \quad (3.1)$$

where

$$-j\bar{k}_i \cdot \bar{r} = jk(x \sin \theta_i \cos \phi_i + y \sin \theta_i \sin \phi_i + z \cos \theta_i). \quad (3.2)$$

Two cases are considered for the formulation and solution: bistatic and monostatic. Bistatic is the most general case. The transmit and receive antenna for the radar are not located at the same position. Monostatic is the case in which the transmit and receive antenna are co-located.

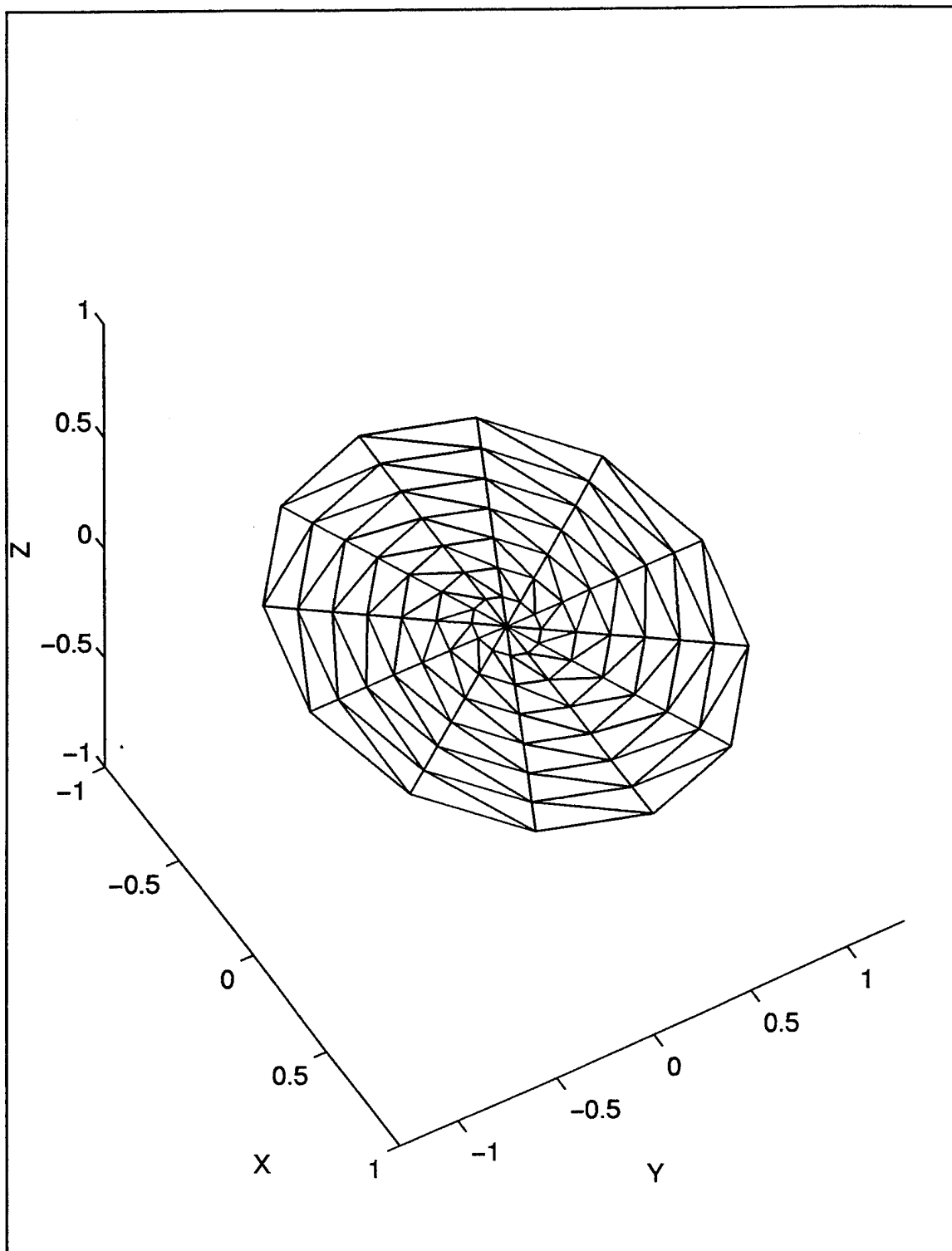


Figure 2. Flat disk in the x-y plane.

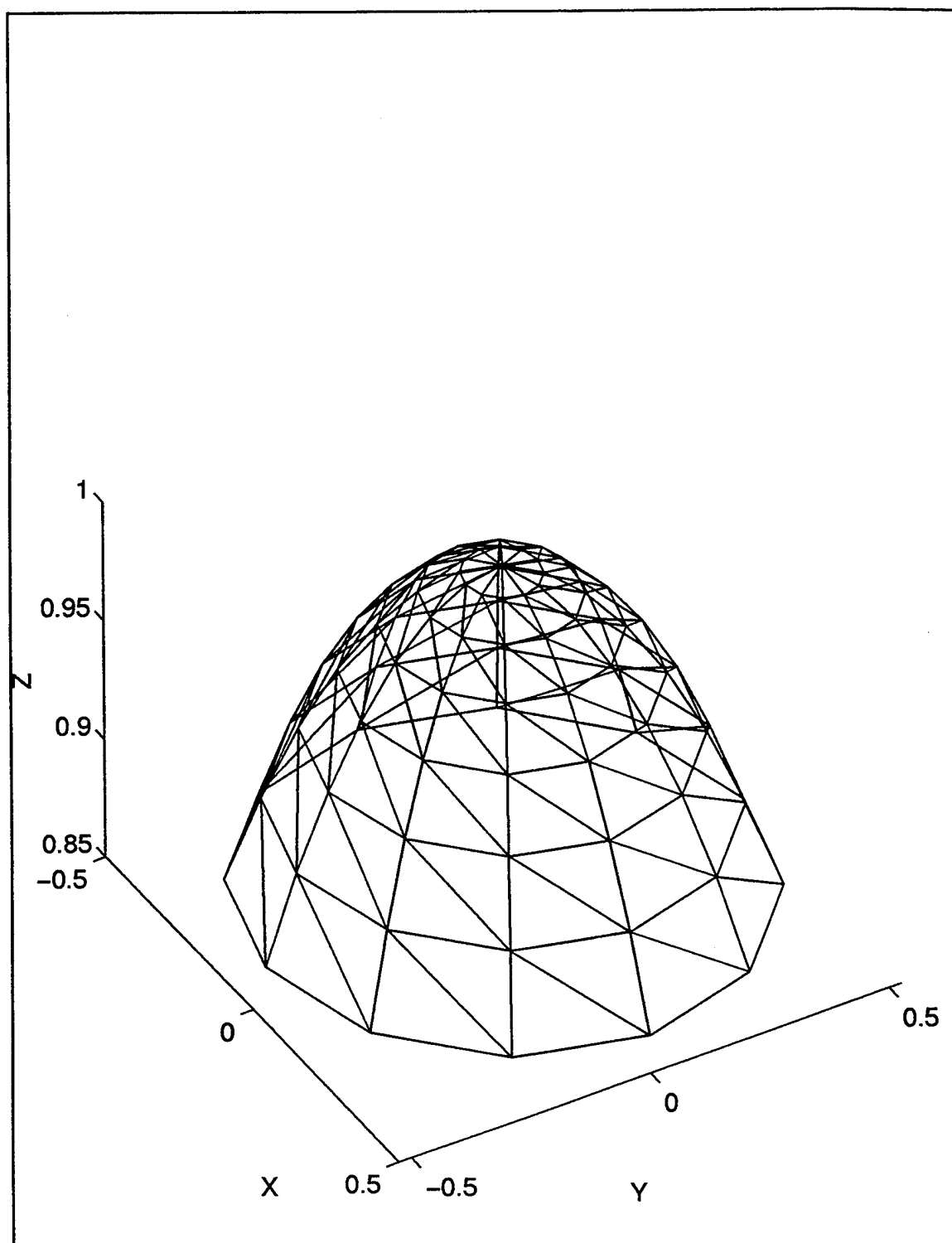


Figure 3. Spherical cap with its base in the x-y plane.

For each case, a flat disk is considered first. The disk is a flat surface with a curved perimeter that requires the use of triangular subsections to model. Next, the more complex shape of a doubly curved surface is solved. The solution for a doubly curved surface is more complex because a transformation of coordinates is required for each triangular subsection. This transformation gives the surface normal in the transformed z axis direction. Also, for the doubly curved surface, the incident wave polarization in the individual triangle coordinate systems is usually not pure TM or TE, even if the polarization is purely TM or TE in the global coordinate system.

## A. BISTATIC CASE

### 1. Flat Disk

For a flat disk in the x-y plane, the normal is always in the z axis direction. Therefore, the boundary condition from equation (2.9) can be written as:

$$\hat{z} \times (\hat{z} \times \bar{E}) = -R_s \bar{J}_s \quad (3.3)$$

where the electric field in the above equation is given by

$$\bar{E}_i = (\hat{\theta} T_{TM} E_{\theta}^i + \hat{\phi} T_{TE} E_{\phi}^i) e^{-j\vec{k}_i \cdot \vec{r}} \quad (3.4)$$

The triple products in equation (3.3) becomes

$$\hat{z} \times (\hat{z} \times \bar{E}) = [(-\hat{x}\cos\theta_i\sin\phi_i + \hat{y}\cos\theta_i\cos\phi_i)T_{TM}E_\theta^i + (-\hat{x}\cos\theta_i\sin\phi_i - \hat{y}\cos\theta_i\cos\phi_i)T_{TE}E_\phi^i]e^{-j\bar{k}_i\bar{r}}. \quad (3.5)$$

By substituting  $T_{TM}$  and  $T_{TE}$  from equations (2.25) and (2.29) into (3.5) and dividing by  $-R_s$ , equation (3.3) can be solved for the current along the surface

$$\bar{J}_s = \left[ \frac{2(-\hat{x}\cos\theta_i\cos\phi_i + \hat{y}\cos\theta_i\sin\phi_i)}{2R_s + \eta_0\cos\theta_i} E_\theta^i + \frac{2(-\hat{x}\sin\phi_i\cos\theta_i - \hat{y}\cos\theta_i\sin\phi_i)}{2R_s\cos\theta_i + \eta_0} E_\phi^i \right] e^{-j\bar{k}_i\bar{r}}. \quad (3.6)$$

The two principal polarizations are considered separately.

#### *a. TM Polarization*

For TM polarization, the  $\phi$  component of the incident field is zero. Therefore,  $\bar{J}_s$  in equation (3.6) simplifies to:

$$\bar{J}_s = \frac{2(-\hat{x}\cos\theta_i\cos\phi_i + \hat{y}\cos\theta_i\sin\phi_i)}{2R_s + \eta_0\cos\theta_i} E_\theta^i e^{-j\bar{k}_i\bar{r}}. \quad (3.7)$$

For use in equation (2.4), equation (3.7) is separated into x and y components

$$J_x = \frac{-2\cos\theta_i\cos\phi_i}{2R_s + \eta_0\cos\theta_i} E_\theta^i e^{-j\bar{k}_i\bar{r}}, \quad (3.8)$$

$$J_y = \frac{2\cos\theta_i\sin\phi_i}{2R_s + \eta_0\cos\theta_i} E_\theta^i e^{-j\bar{k}_i\bar{r}}. \quad (3.9)$$

Equation (2.4) simplifies to:

$$N_{\theta} = \iint_s \left[ \frac{2\cos\theta_i \cos\phi_i \cos\theta \cos\phi}{2R_s + \eta_0 \cos\theta_i} E_{\theta}^i + \frac{2\cos\theta_i \sin\phi_i \cos\theta \sin\phi}{2R_s + \eta_0 \cos\theta_i} E_{\theta}^i e^{jkr'/\cos\psi} e^{-j\vec{k}_i \cdot \vec{r}} dx' dy' \right]. \quad (3.10)$$

Portions of equation (3.10) are not dependant on surface location and can be removed from the integral. Equation (3.10) then reduces to

$$N_{\theta} = 2E_{\theta}^i \cos\theta_i \cos\theta \cos(\phi_i + \phi) \times \iint_s \frac{e^{-j\vec{k}_i \cdot \vec{r}} e^{jkr'/\cos\psi}}{2R_s + \eta_0 \cos\theta_i} dx' dy'. \quad (3.11)$$

The portion of equation (3.11) inside of the integral can be denoted as I for simplicity

$$I = \iint_s \frac{e^{-j\vec{k}_i \cdot \vec{r}} e^{jkr'/\cos\psi}}{2R_s + \eta_0 \cos\theta_i} dx' dy'. \quad (3.12)$$

The resistivity of the material is restricted to be constant on each triangle, but can be a function of location on the surface of the object. Therefore, it must remain within the integral. Thus the resistivity function can be defined as a series of pulses with unknown coefficients

$$R_s(x_o, y_o) = \sum_{o=1}^N r_o f_c(x_o, y_o) \quad (3.13)$$

where  $c$  is the triangle number and  $N$  is the total number of triangles on the surface of the object. The coefficients  $r_c$  are the unknown expansion coefficients and  $f_c$  are the step functions

$$f_c = \begin{cases} 1, & x_o, y_o \in S_c \\ 0, & \text{otherwise} \end{cases} \quad (3.14)$$

where  $S_c$  is the area of triangle  $c$ . Substituting equation (3.13) into (3.12) gives

$$I = \iint_s \frac{e^{-j\vec{k}_i \cdot \vec{r}} e^{j\vec{k}_r \cdot \cos \psi}}{2 \sum_{o=1}^N r_o f_c + \eta_o \cos \theta_i} dx' dy' . \quad (3.15)$$

Breaking the integral into a sum of integrals over the individual triangles gives

$$I = \sum_{o=1}^N \iint_{s_c} \frac{e^{-j\vec{k}_i \cdot \vec{r}} e^{j\vec{k}_r \cdot \cos \psi}}{2 r_c + \eta_o \cos \theta_i} dx' dy' \equiv \sum_{o=1}^N I_o . \quad (3.16)$$

The  $c^{\text{th}}$  term of the sum is

$$I_c = \frac{\iint_{S_c} e^{-j\vec{k}_i \cdot \vec{r}} e^{jkr' \cos \psi} dx' dy'}{2r_c + \eta_o \cos \theta_i} \quad (3.17)$$

The denominator of equation (3.17) can be defined as

$$a_o = \frac{1}{2r_c + \eta_o \cos \theta_i} \quad (3.18)$$

The integrals over the individual triangles can be reduced to closed form as described by Moreira and Prata. [Ref. 6] In general,

$$I_c = 2S_o e^{jD_o} \left[ \frac{e^{jD_p} C_o}{D_p(D_q - D_p)} - \frac{e^{jD_q} C_o}{D_q(D_q - D_p)} - \frac{C_o}{D_q D_p} \right] \quad (3.19)$$

In equation (3.19), the C and D coefficients are given by the following equations:

$$C_o = A_{c,3} \quad (3.20)$$

$$D_o = kB_{c,3} \quad (3.21)$$

$$D_p = k(B_{c,1} - B_{c,3}) \quad (3.22)$$

$$D_q = k(B_{c,2} - B_{c,3}) \quad (3.23)$$

where  $A_{c,i}$  is the amplitude value of the integrand of (3.17) at the  $i^{\text{th}}$  vertex of triangle  $c$ , and  $kB_{c,i}$  is its phase. The quantities are defined in Figure 4. The primed coordinates are the local Cartesian coordinates with  $z''$  normal to the patch.

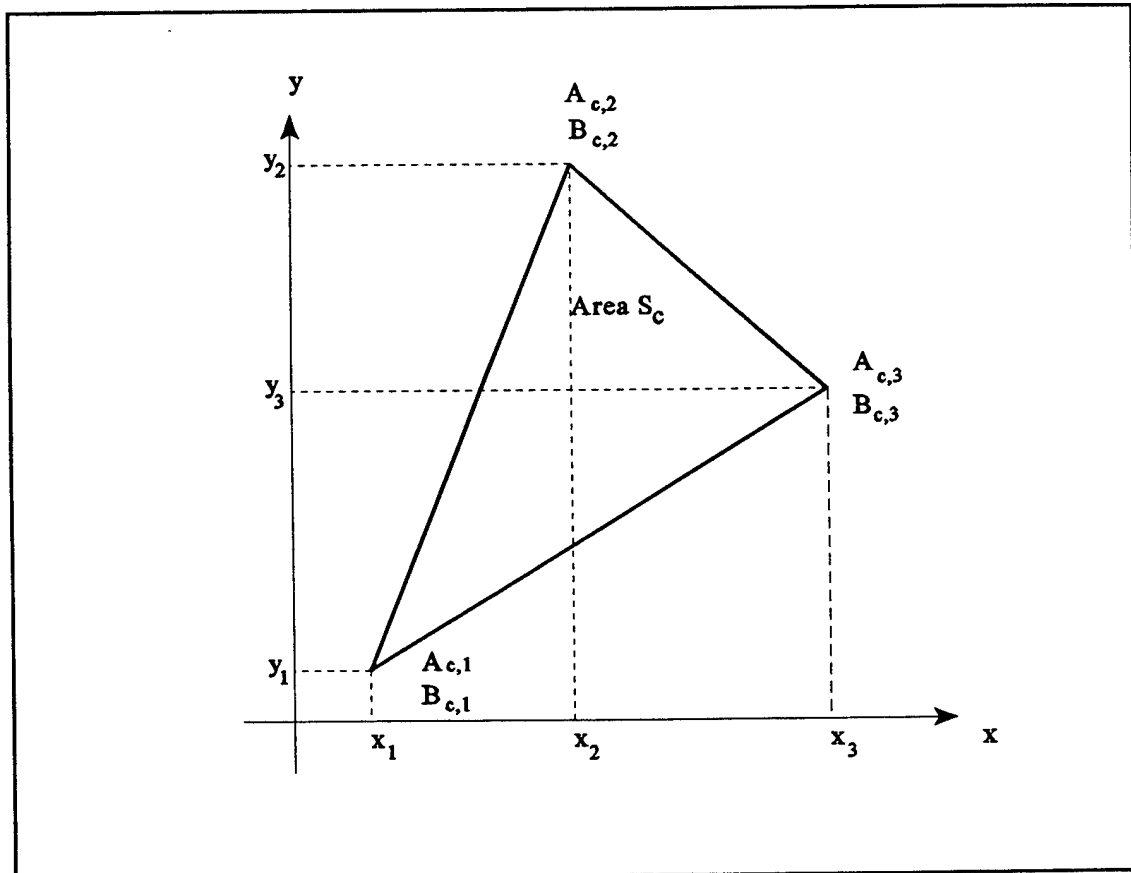


Figure 4. Integration cell geometry.

Equation (3.19) has singularities which can be removed by using Taylor series expansions for four special cases.

Case 1,  $|D_p| < Lt$  and  $|D_q| \geq Lt$ :

$$I_o = 2S_o \frac{e^{jD_o}}{jD_q} \sum_{n=0}^{\infty} \frac{(jD_p)^n}{n!} \left[ -\frac{C_o}{n+1} + e^{jD_q} C_o G(n, -D_q) \right] . \quad (3.24)$$

Case 2,  $|D_p| < Lt$  and  $|D_q| < Lt$ :

$$I_o = 2S_o e^{jD_o} \sum_{n=0}^{\infty} \sum_{m=0}^{\infty} \frac{(jD_p)^n (jD_q)^m}{(n+m+1)!} C_o . \quad (3.25)$$

Case 3,  $|D_p| \geq Lt$  and  $|D_q| < Lt$ :

$$I_o = 2S_o e^{jD_o} e^{jD_p} \sum_{n=0}^{\infty} \frac{(jD_q)^n}{n!} \left[ \frac{C_o}{n+1} G(n+1, -D_p) \right] . \quad (3.26)$$

Case 4,  $|D_p| \geq Lt$ ,  $|D_q| \geq Lt$ , and  $|D_p - D_q| < Lt$ :

$$I_o = 2S_o \frac{e^{jD_o}}{jD_q} \sum_{n=0}^{\infty} \frac{[j(D_p - D_q)]^n}{n!} \left[ -C_o G(n, D_q) + \frac{e^{jD_q} C_o}{(n+1)} \right] . \quad (3.27)$$

In the above equations,  $n$  and  $m$  are the series terms,  $Lt$  is a small number that determines the region of applicability of the series approximation, and  $G$  is a function of the form:

$$G(n, w) = \int_0^1 s^n e^{jws} ds . \quad (3.28)$$

For the calculations in this thesis, values of  $Lt=.005$  and  $m=n=2$  were sufficient.

Substitution of equations (3.16) and (3.19) into (3.10) yields

$$N_{\theta} = 2E_{\theta}^i \cos\theta_i \cos\theta \cos(\phi_i - \phi) \sum_{c=1}^N a_c I_c . \quad (3.29)$$

From equation (2.2), the expression for the co-polarized scattered field is

$$E_{\theta\theta}^s = \frac{-jk\eta_o e^{-jkr}}{2\pi r} E_{\theta}^i \cos\theta_i \cos\theta \cos(\phi_i - \phi) \sum_{c=1}^N a_c I_c . \quad (3.30)$$

Finally, using  $I$  in place of the sum, the co-polarized RCS is

$$\sigma_{\theta\theta} = \frac{(k\eta_o)^2}{\pi} |\cos\theta_i \cos\theta \cos(\phi_i - \phi) I|^2 . \quad (3.31)$$

To calculate the cross-polarized scattered field, equation (2.5) is used and the same procedure employed to obtain the co-polarized RCS is followed. Equation (2.5) reduces to

$$N_{\phi} = 2E_{\theta}^i \cos\theta_i \sin(\phi - \phi_i) I . \quad (3.32)$$

Equation (2.3) for the scattered field becomes

$$E_{\phi\theta}^s = \frac{-jk\eta_o e^{-jkr}}{2\pi r} E_{\theta}^i \cos\theta_i \sin(\phi - \phi_i) I \quad (3.33)$$

and the cross-polarized RCS is

$$\sigma_{\phi\theta} = \frac{(k\eta_o)^2}{\pi} |\cos\theta_i \sin(\phi - \phi_i) I|^2 . \quad (3.34)$$

**b. TE Polarization**

For TE polarization, the  $\theta$  component of the incident field is zero. Therefore,  $\bar{J}_s$  in equation (3.6) simplifies to

$$\bar{J}_s = \frac{2(-\hat{x}\sin\phi_i\cos\theta_i - \hat{y}\cos\theta_i\sin\phi_i)}{2R_i\cos\theta_i + \eta_o} E_\phi^i e^{-j\bar{k}_i \cdot \bar{r}} . \quad (3.35)$$

For use in equation (2.4), (3.35) is separated into x and y components.

$$J_x = \frac{-2(\sin\phi_i\cos\theta_i)}{2R_i\cos\theta_i + \eta_o} E_\phi^i e^{-j\bar{k}_i \cdot \bar{r}} , \quad (3.36)$$

$$J_y = \frac{-2(\cos\theta_i\sin\phi_i)}{2R_i\cos\theta_i + \eta_o} E_\phi^i e^{-j\bar{k}_i \cdot \bar{r}} . \quad (3.37)$$

Equation (2.4) simplifies to

$$N_\theta = -2(\cos\theta\cos\theta_i\sin(\phi - \phi_i)) \iint \frac{e^{j\bar{k}r'\cos\psi} e^{-j\bar{k}_i \cdot \bar{r}}}{2R_i\cos\theta_i + \eta_o} dx' dy' . \quad (3.38)$$

The equation for  $I$  corresponding to equation (3.14) becomes

$$I = \iint \frac{e^{jk_r' \cos \psi} e^{-j\vec{k}_i \cdot \vec{r}}}{2R_i \cos \theta_i + \eta_o} dx' dy' . \quad (3.39)$$

Equation (3.19) for  $I_c$  remains the same. However, the denominator is not the same and therefore, a new variable  $b_o$  is defined:

$$b_o = \frac{1}{2R_i \cos \theta_i + \eta_o} . \quad (3.40)$$

The equation for the cross-polarized scattered field becomes

$$E_{\theta\phi}^s = \frac{-jk\eta_o e^{-jk_r}}{2\pi r} E_{\phi}^i \cos \theta_i \cos \theta \sin(\phi - \phi_i) I \quad (3.41)$$

and the cross-polarized RCS is

$$\sigma_{\theta\phi} = \frac{(k\eta_o)^2}{\pi} |\cos \theta_i \cos \theta \sin(\phi - \phi_i) I|^2 . \quad (3.42)$$

The scattered field for the co-polarized direction is derived in a similar manner yielding

$$E_{\phi\phi}^s = \frac{-jk\eta_o e^{-jk_r}}{2\pi r} E_{\phi}^i \cos \theta_i \cos(\phi - \phi_i) I \quad (3.43)$$

and

$$\sigma_{\phi\phi} = \frac{(k\eta_o)^2}{\pi} |\cos\theta_i \cos(\phi - \phi_i) I|^2 . \quad (3.44)$$

*c. Arbitrary Polarization*

The most general incident polarization is a combination of TM and TE components. The total scattered field in the  $\theta$  direction is

$$E_{\theta}^s = E_{\theta\theta}^s + E_{\theta\phi}^s \quad (3.45)$$

or,

$$E_{\theta}^s = \frac{-jk\eta_o e^{-jkr}}{2\pi r} E_{\theta}^i [\cos\theta_i [\cos\theta \cos(\phi - \phi_i) + \sin(\phi - \phi_i)]] . \quad (3.46)$$

And the total scattered field in the  $\phi$  direction is

$$E_{\phi}^s = E_{\phi\theta}^s + E_{\phi\phi}^s \quad (3.47)$$

or,

$$E_{\phi}^s = \frac{-jk\eta_o e^{-jkr}}{2\pi r} E_{\phi}^i [\cos\theta_i [\cos\theta \sin(\phi - \phi_i) + \cos(\phi - \phi_i)]] . \quad (3.48)$$

Equations (3.47) and (3.48) can now be put into a matrix form.

$$\begin{bmatrix} E_{\theta}^s \\ E_{\phi}^s \end{bmatrix} = \begin{bmatrix} A_{\theta\theta} & A_{\theta\phi} \\ A_{\phi\theta} & A_{\phi\phi} \end{bmatrix} \begin{bmatrix} S_{\theta} \\ S_{\phi} \end{bmatrix} \quad (3.49)$$

where

$$A_{\theta\theta} = \frac{-jk\eta_o e^{-jkr}}{2\pi r} E_{\theta}^i \cos\theta_i \cos\theta \cos(\phi - \phi_i) , \quad (3.50)$$

$$A_{\theta\phi} = \frac{-jk\eta_o e^{-jkr}}{2\pi r} E_{\phi}^i \cos\theta_i \cos\theta \sin(\phi - \phi_i) , \quad (3.51)$$

$$A_{\phi\theta} = \frac{-jk\eta_o e^{-jkr}}{2\pi r} E_{\theta}^i \cos\theta_i \sin(\phi - \phi_i) , \quad (3.52)$$

$$A_{\phi\phi} = \frac{-jk\eta_o e^{-jkr}}{2\pi r} E_{\phi}^i \cos\theta_i \cos(\phi - \phi_i) , \quad (3.53)$$

$$S_{\theta} = \sum_{c=1}^N a_c I_{\theta} , \quad (3.54)$$

and

$$S_{\phi} = \sum_{c=1}^N b_c I_c . \quad (3.55)$$

The resistivity of each triangle is embedded in  $a_c$  and  $b_c$  via equations (3.54) and (3.55).

## 2. Doubly Curved Surfaces

For a doubly curved surface, the surface normal vector of each triangular subsection can be different. The equations (3.19) through (3.27) still hold if the local triangle coordinates are used. Therefore a transformation of the coordinates must be performed for each triangular facet on the surface from the global system  $(x,y,z)$  to the local system  $(x'',y'',z'')$  as shown in Figure 5. The  $z''$  axis is in the same direction as the facet normal  $\hat{n}_c$ . After the transformation of coordinates, the scattering calculations are made for each triangle, the fields summed over all triangles, and then a transformation is made back to the original (global) coordinates.

The incident field is first converted to global Cartesian coordinates [Ref. 4]

$$\begin{bmatrix} E_x^i \\ E_y^i \\ E_z^i \end{bmatrix} = \begin{bmatrix} \cos\phi\sin\theta & \cos\theta\cos\phi & -\sin\phi \\ \sin\theta\sin\phi & \cos\theta\sin\phi & \cos\phi \\ \cos\theta & -\sin\theta & 0 \end{bmatrix} \begin{bmatrix} E_r^i \\ E_{\theta}^i \\ E_{\phi}^i \end{bmatrix} . \quad (3.56)$$

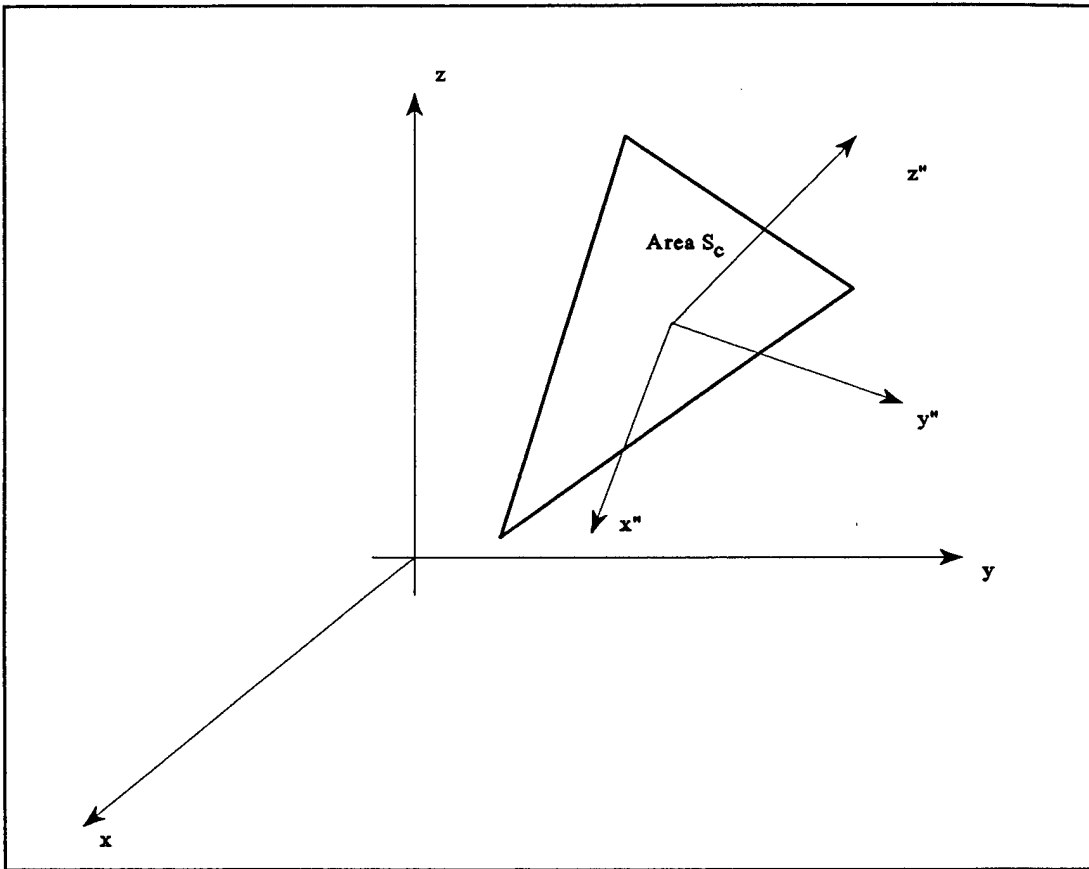


Figure 5. Transformation of coordinates from a global  $(x,y,z)$  to a local  $(x'',y'',z'')$  system for triangle c.

Next, a rotation about the  $z$  axis is performed to give a new coordinate system  $(x',y',z')$ . Then a rotation about the  $y'$  axis is done to give the local coordinate system of triangle c  $(x'',y'',z'')$

$$\begin{bmatrix} x'' \\ y'' \\ z'' \end{bmatrix} = \begin{bmatrix} \cos\alpha_c & \sin\alpha_c & 0 \\ -\sin\alpha_c & \cos\alpha_c & 0 \\ 0 & 0 & 1 \end{bmatrix} \begin{bmatrix} \cos\beta_c & 0 & -\sin\beta_c \\ 0 & 1 & 0 \\ \sin\beta_c & 0 & \cos\beta_c \end{bmatrix} \begin{bmatrix} x \\ y \\ z \end{bmatrix}. \quad (3.57)$$

The angle  $\alpha_c$  is the angle of rotation about the z axis, and the angle  $\beta_c$  is the angle of rotation about the y' axis, where

$$\alpha_c = \tan^{-1} \left( \frac{\hat{n}_c \times \hat{y}}{\hat{n}_c \times \hat{x}} \right) \quad (3.58)$$

and

$$\beta_c = \cos^{-1}(\hat{n}_c \times \hat{z}) . \quad (3.59)$$

The incident field is also transformed to the local coordinate system using the same matrices as in equation (3.57). After all transformations are complete, equations (3.45) through (3.55) are applied. Once the scattered field for each triangle is calculated, it is transformed back to the global coordinate system and the fields from all triangles are summed vectorially. Equations (3.31), (3.34), (3.42), and (3.45) are then used to calculate the total RCS of the surface.

## B. MONOSTATIC CASE

For a monostatic radar,  $\phi_i = \phi$  and  $\theta_i = \theta$  and the scattered fields reduce to

$$E_\theta^s = \frac{-jk\eta_0 e^{-jkr}}{2\pi r} E_\theta^i \cos^2 \theta \quad (3.60)$$

and

$$E_{\phi}^s = \frac{-jk\eta_o e^{-jkr}}{2\pi r} E_{\phi}^i \cos\theta \quad (3.61)$$

In equations (3.60) and (3.61),  $I$  is still given by equations (3.15) and (3.38). Recall that  $a_c$  and  $b_c$  are dependant on  $\theta_i$  and location on the surface. In order to synthesize an equation for resistivity,  $a_c$  and  $b_c$  cannot be dependant on  $\theta_i$ . This implies that the surface composition must change for each incidence angle (ie., an adaptive target). One approximation that eliminates the dependance on  $\theta_i$  is to consider  $\cos\theta_i=1$ . In this case,

$$a_c = b_c = \frac{1}{2r_c + \eta_o} \quad (3.62)$$

and equations (3.60) and (3.61) reduce to

$$E_{\theta}^s = \frac{-jk\eta_o e^{-jkr}}{2\pi r} E_{\theta}^i I \quad (3.63)$$

$$E_{\phi}^s = \frac{-jk\eta_o e^{-jkr}}{2\pi r} E_{\phi}^i I \quad (3.64)$$

### C. SYNTHESIS EQUATIONS

In applying the synthesis procedure, only the monostatic case is considered. The scattered field at various angles is

known from equations (3.63) and (3.64). For synthesis, the scattered fields in these equations are known. The values for  $I$  and subsequently  $a_c$  ( $=b_c$ ) are to be determined. Faros has shown that in providing  $E_\theta^s$  and  $E_\phi^s$  uniform sampling of the field in direction cosine space (DCS) leads to less numerical errors than sampling in  $\theta$  and  $\phi$ . [Ref. 5] Therefore, it is more convenient to work in DCS. Figure 6 shows the domain of DCS. The visible region is the area within the unit circle.

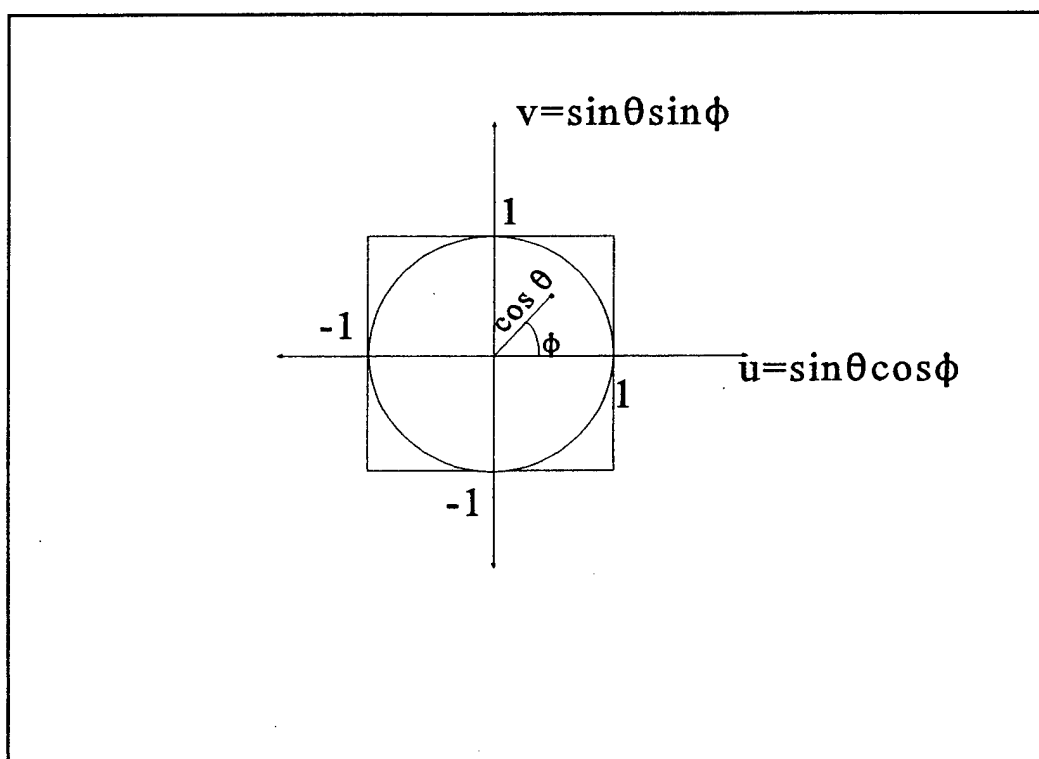


Figure 6. Direction cosine space.

To generate field values for the left sides of equations (3.63) and (3.64), DCS is divided into squares of area  $du$  by  $dv$ . There are  $N_u$  divisions along the  $u$  axis and  $N_v$  divisions along the  $v$  axis. The center of each square is the sample point for calculating the scattered field. This gives a total of  $N_u$  by  $N_v$  samples of the scattered field. However, only the points within the visible region are valid for use in the synthesis equations. The number of points inside the visible region is defined to be  $N$ . The angles  $\theta$  and  $\phi$  for use in calculating the scattered field are found from

$$\theta = \sin^{-1}(u^2 + v^2) \quad (3.65)$$

$$\phi = \tan^{-1}\left(\frac{v}{u}\right) . \quad (3.66)$$

The unknowns in the synthesis problem are the expansion coefficients,  $a_k$ . There is one value of  $a_k$  for each triangular subsection. Let  $a$  be a vector of  $N$  elements representing  $N$  unknowns. In order for the equation to be solved uniquely,  $N$  unknowns require  $N$  equations and, therefore, the number of samples of the scattered field must also be  $N$ . A matrix equation follows from equations (3.15), (3.60), and (3.61):

$$\begin{bmatrix} E_1^s \\ E_2^s \\ \vdots \\ E_N^s \end{bmatrix} = \begin{bmatrix} X_{11} & X_{12} & \dots & X_{1N} \\ X_{21} & X_{22} & \dots & X_{2N} \\ \vdots & \vdots & & \vdots \\ X_{N1} & X_{N2} & \dots & X_{NN} \end{bmatrix} \begin{bmatrix} a_1 \\ a_2 \\ \vdots \\ a_N \end{bmatrix} \quad (3.67)$$

or

$$E = Xa \quad (3.68)$$

where

$$E_n^s = E^s(\theta_n, \phi_n) = E^s(u_n, v_n), \quad (3.69)$$

$$X_{nc} = \left[ \frac{-j\eta_0 e^{-jk_r}}{2\pi r} (\hat{\theta} E_\theta^i + \hat{\phi} E_\phi^i) I_0 \right] \Big|_{u=u_n, v=v_n}, \quad (3.70)$$

and  $c, n=1, 2, \dots, N$ .

The  $X$  matrix is square and can be inverted and used to solve for the  $a$  matrix

$$\begin{bmatrix} a_1 \\ a_2 \\ \vdots \\ a_N \end{bmatrix} = \begin{bmatrix} X_{11} & X_{12} & \dots & X_{1N} \\ X_{21} & X_{22} & \dots & X_{2N} \\ \vdots & \vdots & & \vdots \\ X_{N1} & X_{N2} & \dots & X_{NN} \end{bmatrix}^{-1} \begin{bmatrix} E_1^s \\ E_2^s \\ \vdots \\ E_N^s \end{bmatrix}. \quad (3.71)$$

Then using equation (3.62), each element in the  $a$  matrix is

used to solve for the resistivity over each triangle,

$$r_c = \frac{1}{2} \left[ \frac{1}{a_c} - \eta_o \right] . \quad (3.72)$$

Equation (3.72) represents the synthesis equation for calculating the resistivity of an object given the required RCS.



## IV. COMPUTER IMPLEMENTATION AND DATA ANALYSIS

This chapter discusses the computer coding of the equations derived from Chapters II and III. The first sections cover the calculation of the RCS, while the second half addresses the synthesis calculation.

### A. RCS FROM THE SCATTERED FIELD

Using equation (2.1), the RCS can be calculated from a scattered field. The incident field is assumed TM polarized and the monostatic RCS is calculated for the scattered field obtained using equations (3.60) and (3.61). A listing of the program POTEEST is included in the appendix. It should be noted that POTEEST calls several subroutines which are also included in the appendix.

A  $1\lambda \times 1\lambda$  flat PEC plate was used as the initial test case. The patch model of the plate is shown in Figure 7. In Figure 8, the approximate (PO) results are compared to the method of moments (exact) results. The specular lobe was within a few dB, but the sidelobes are slightly larger in the exact results. This is due to the fact that the approximation used in equation (3.3) neglects any traveling waves.

The second test was to place some resistivity on the surface of the plate. First, a constant resistivity of 377 ohms was used. A comparison of the PO and MOM results is seen in Figure 9. Note that with a resistance on the surface, the sidelobe differences decrease.

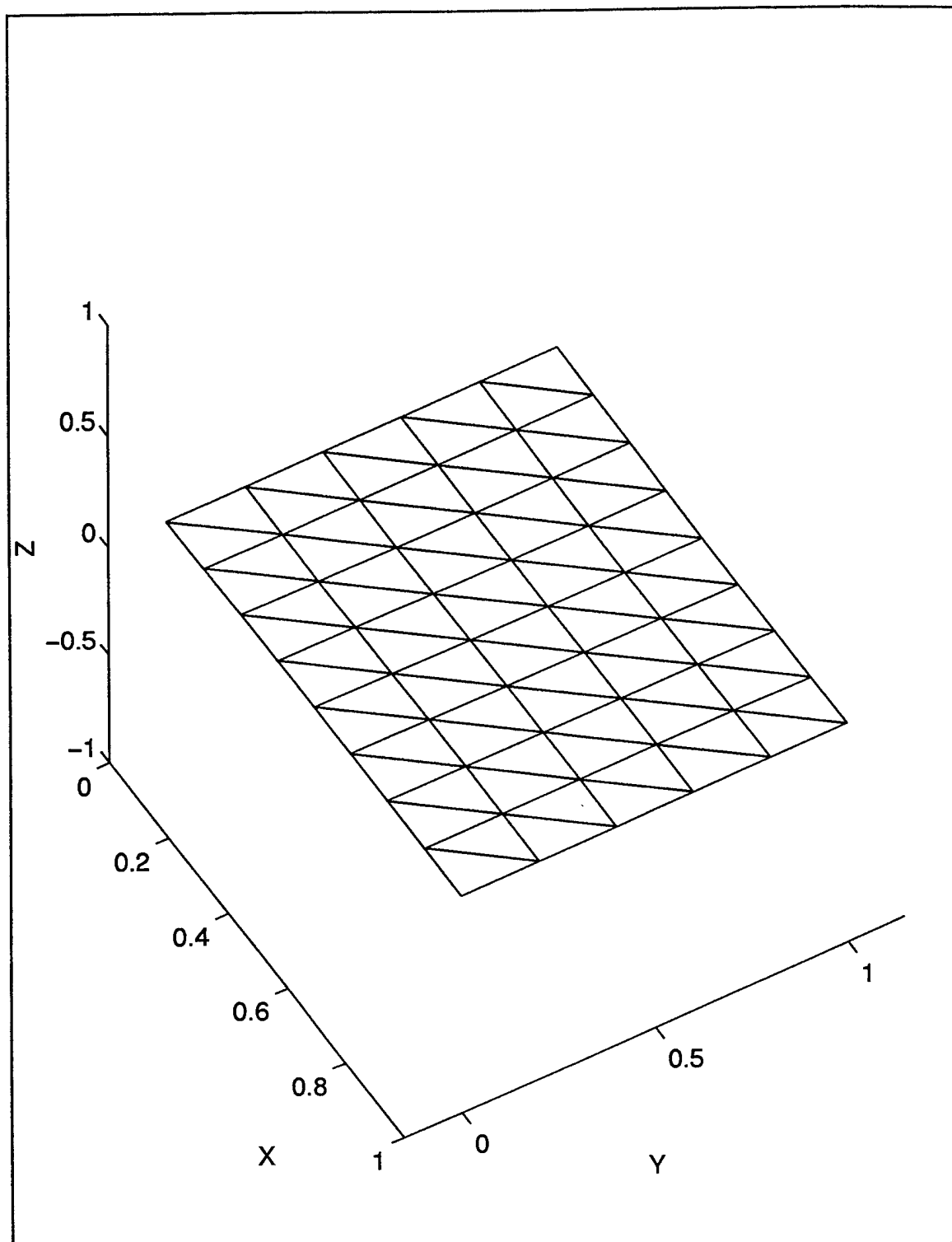


Figure 7. Flat plate in the x-y plane.

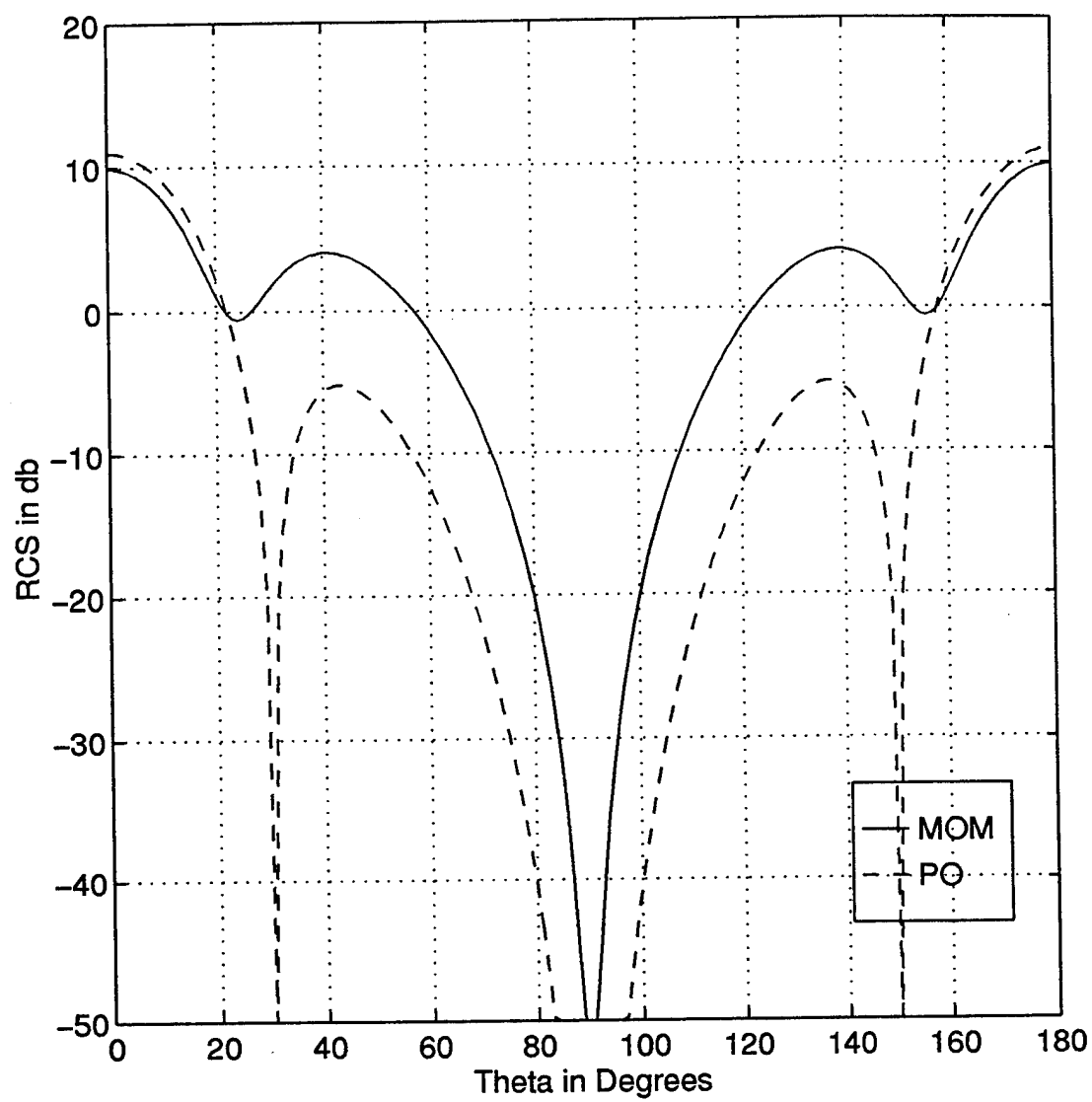


Figure 8. RCS of a PEC flat plat (TM polarized incident wave, monostatic).

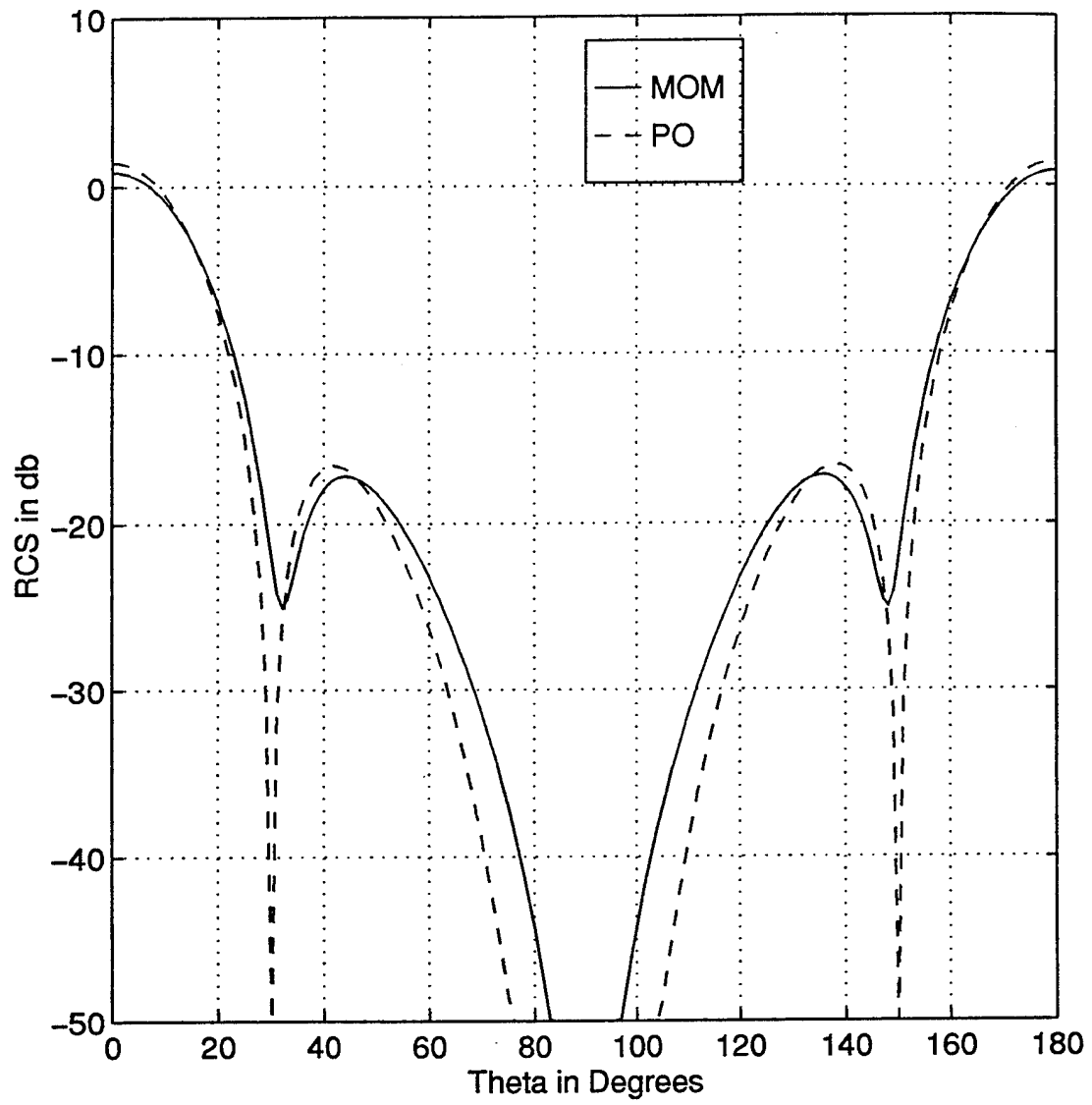


Figure 9. RCS of a flat plate with surface resistivity of  $377 \Omega/\square$  (TM polarized incident wave, monostatic).

The final test was to increase the resistivity linearly from 0 to 377  $\Omega/\square$  from the center of the plate to the edges. This was done using the equation

$$R_o = 377(x_c^2 + y_c^2) \quad (4.1)$$

where  $x_c$  and  $y_c$  are the midpoints of triangle c. Equation (4.1) is for a flat surface laying in the x-y plane, centered at the origin. The results are shown in Figure 10.

The next step was to look at a flat disk and a spherical cap with and without resistivity to establish the accuracy of PO relative to MOM. The models used for a flat disk and a spherical cap are shown in Figures 2 and 3, respectively. The results for a flat disk are shown in Figures 11 through 13. Figure 11 is the RCS of a conducting disk, Figure 12 for a disk with constant resistivity of 377  $\Omega/\square$ , and Figure 13 is for a disk with resistivity given by equation (4.1). Figures 14 through 16 are the results for a spherical cap. Figure 14 shows the RCS for a PEC cap, Figure 15 for constant resistivity of 377  $\Omega/\square$  across the cap, and Figure 16 for linear resistivity using

$$R_o = 377 \frac{t_c}{t_{max}} \quad (4.2)$$

where  $t_c$  is the arclength from the pole to the center of triangle c and,  $t_{max}$  is the total arclength from the pole to the base of the cap.

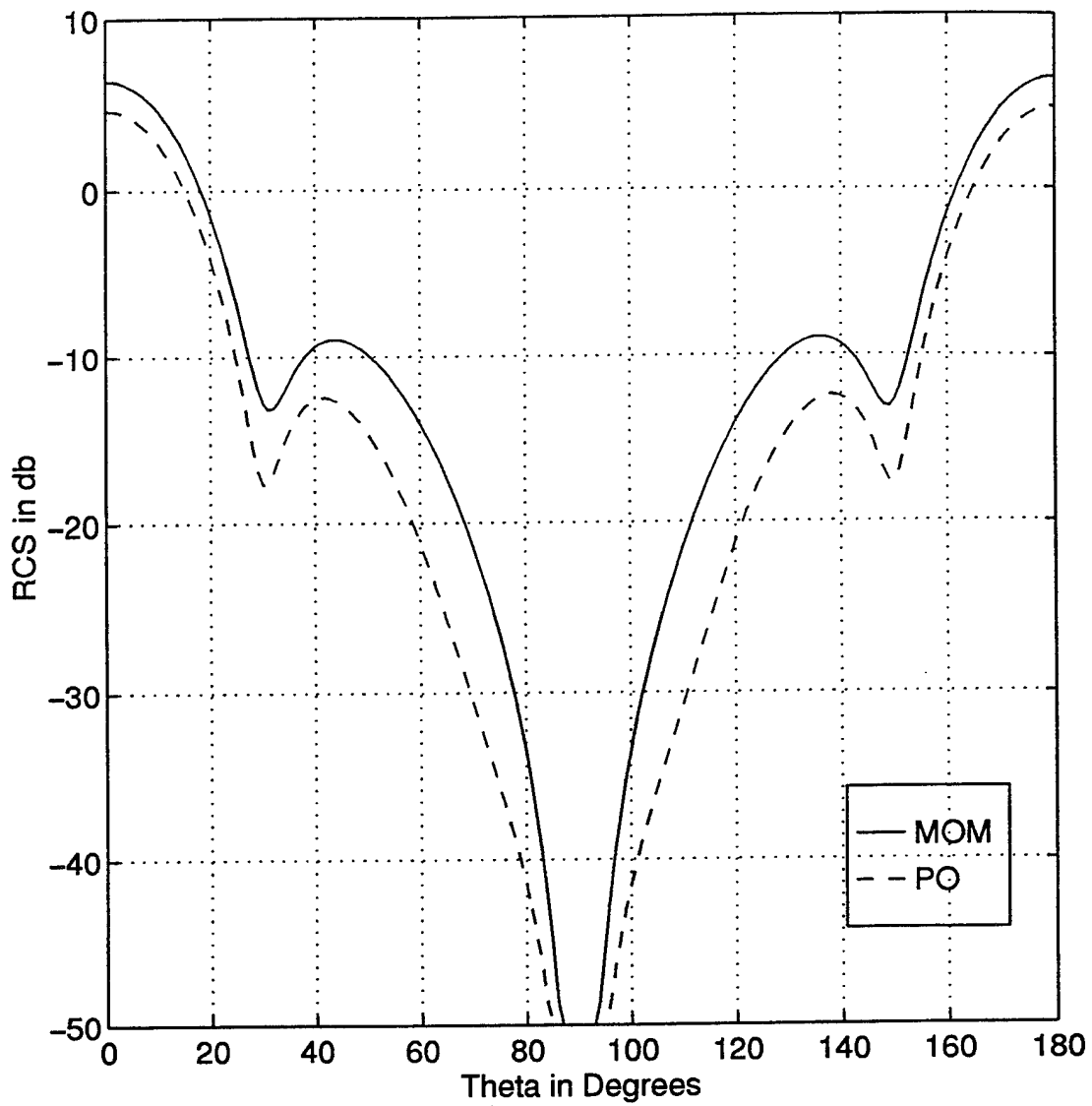


Figure 10. RCS of a flat plate with surface resistivity given by equation (4.1)(TM polarized incident wave, monostatic).

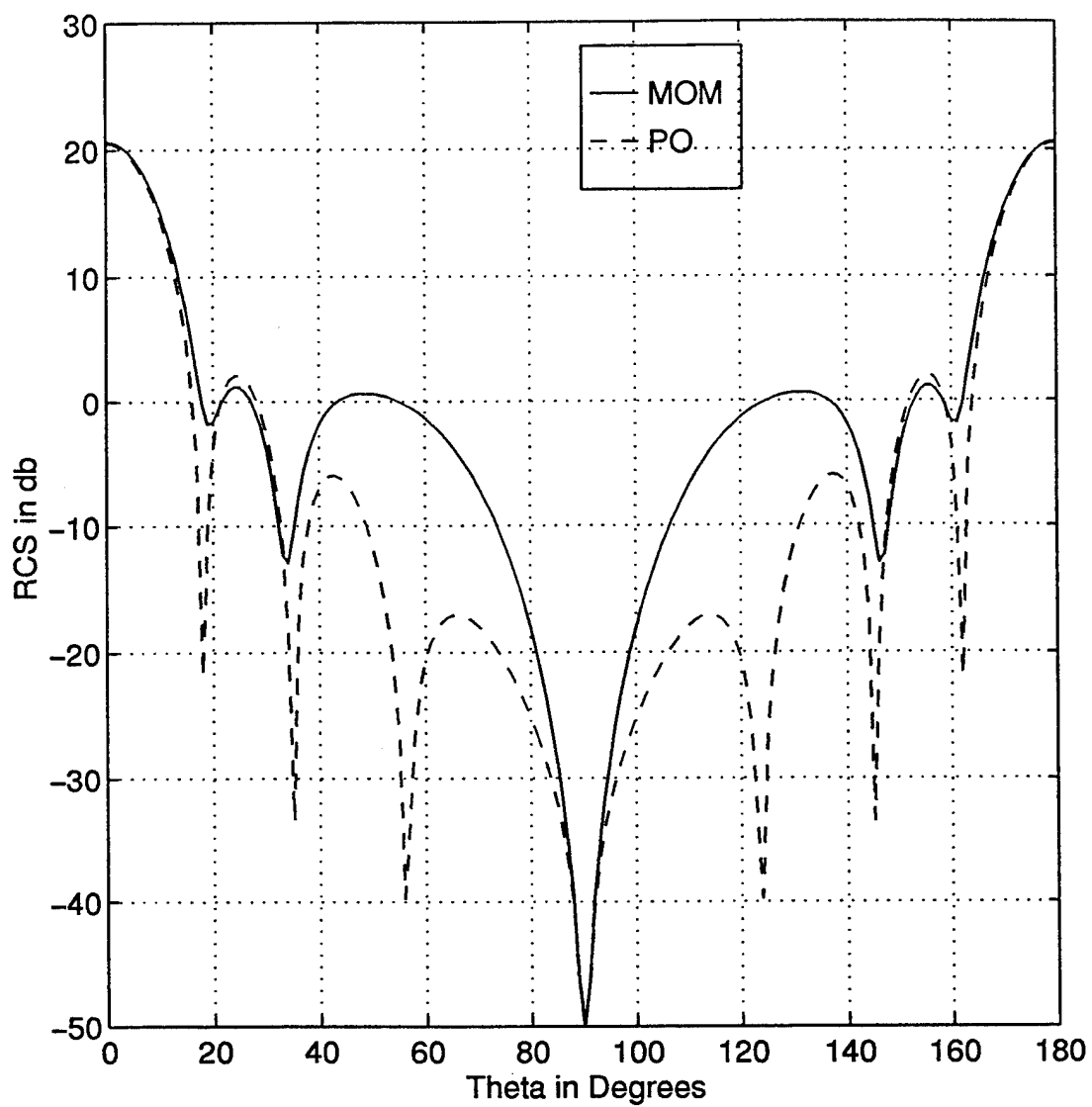


Figure 11. RCS of a PEC flat disk (TM polarized incident wave, monostatic).

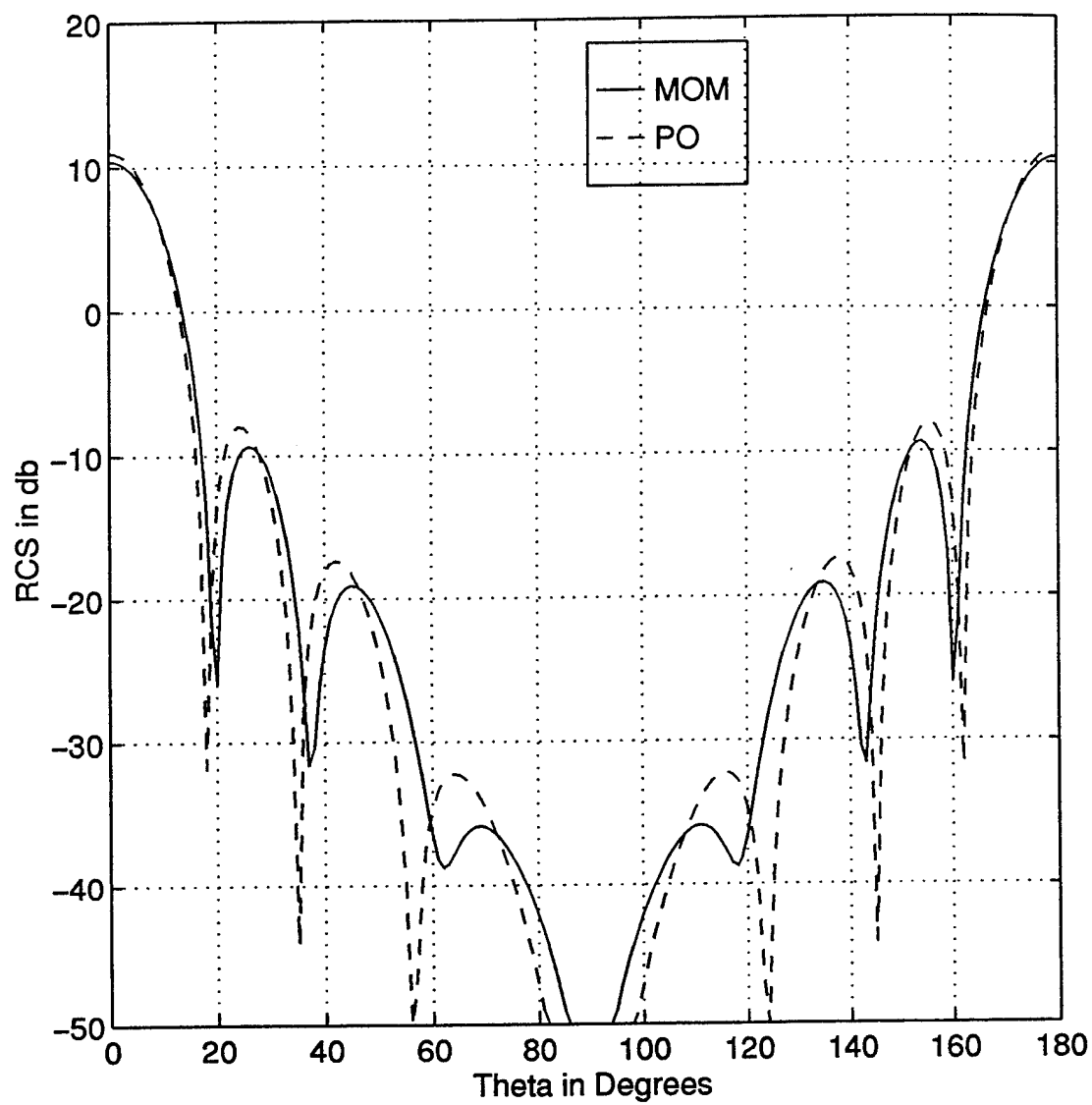


Figure 12. RCS of a flat disk with  $377 \Omega/\square$  surface resistivity(TM polarized incident wave, monostatic).

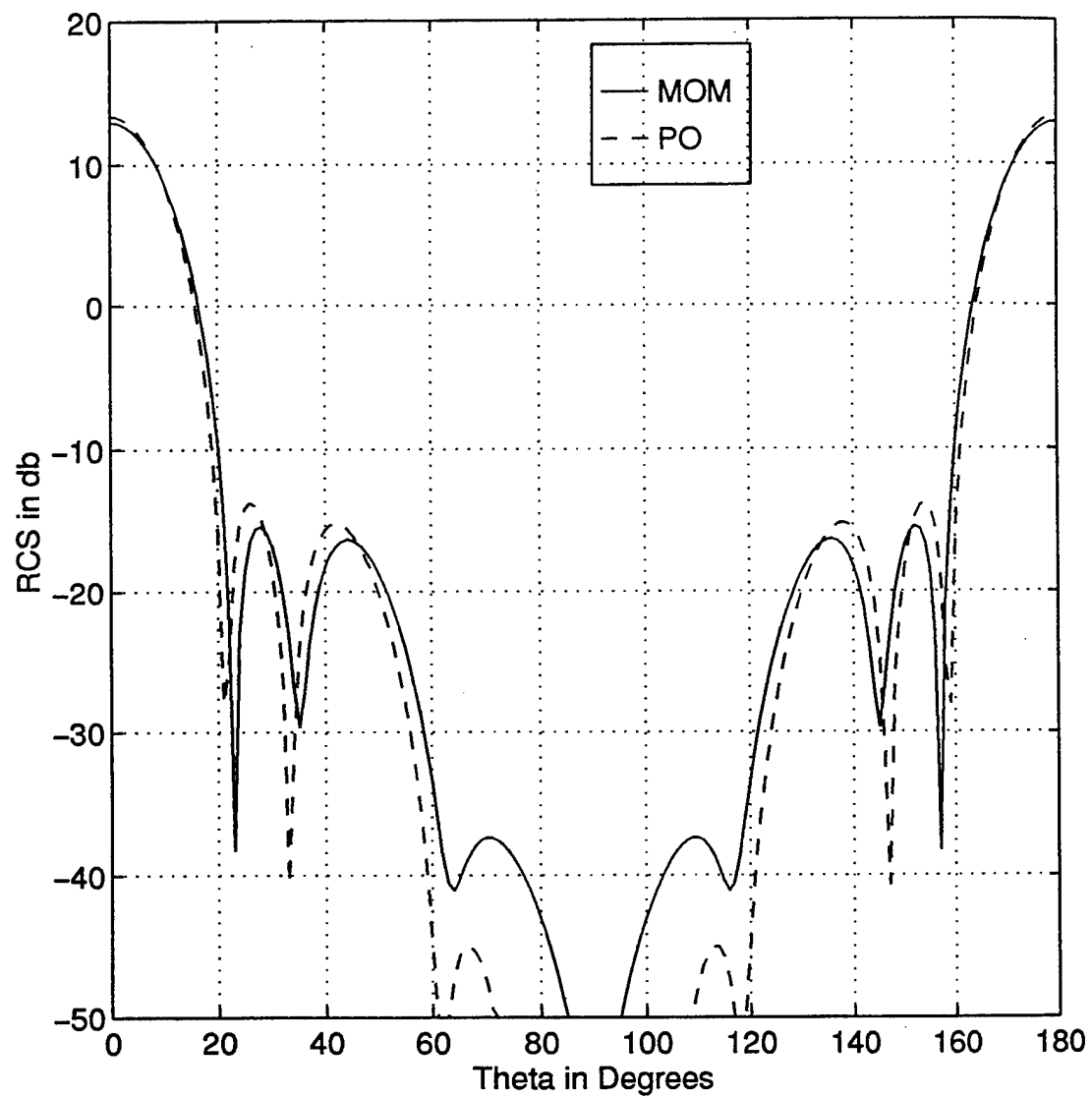


Figure 13. RCS of a flat disk with surface resistivity given by equation (4.1) (TM polarized incident wave, monostatic).

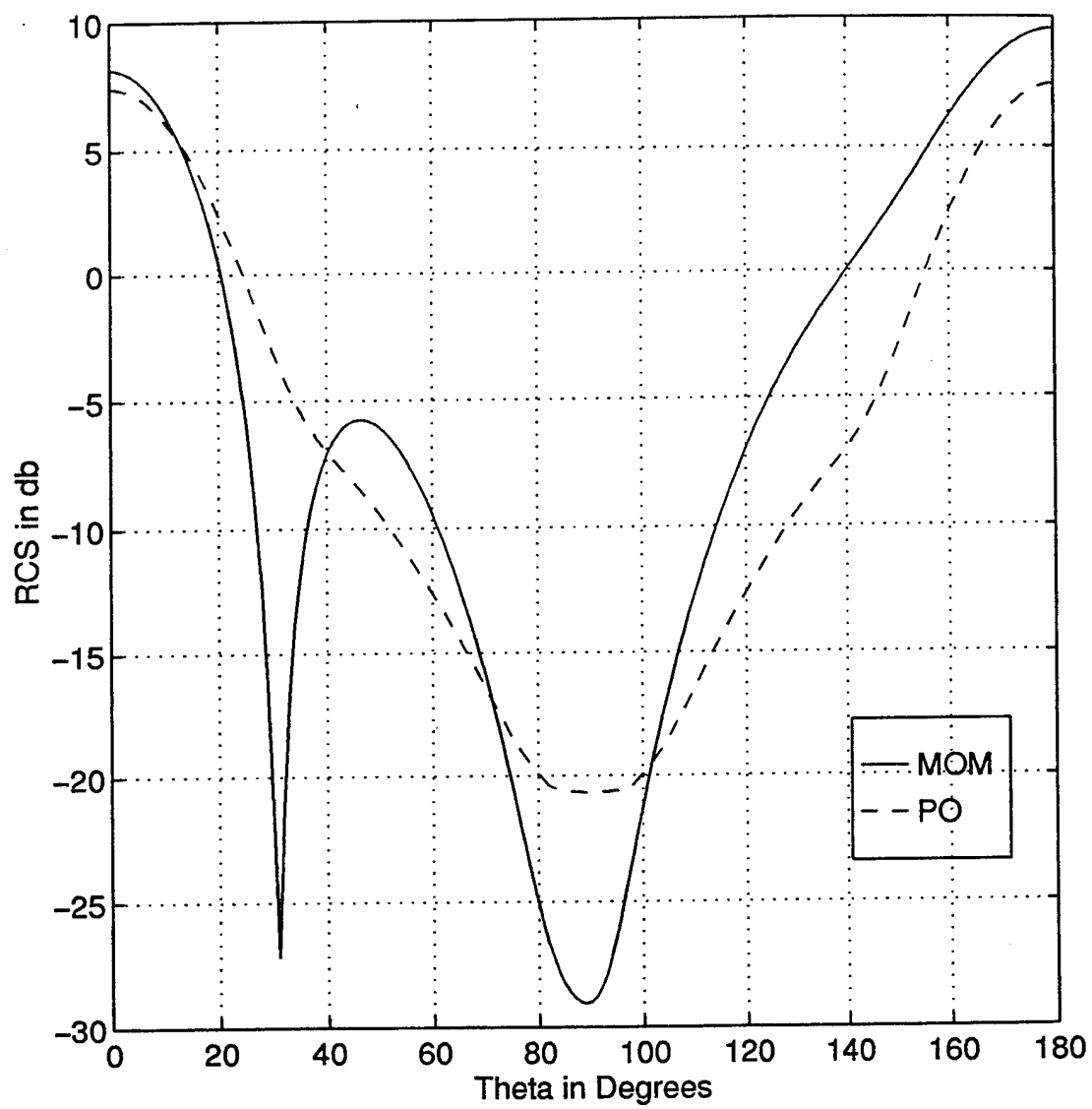


Figure 14. RCS of a PEC spherical cap (TM polarized incident wave, monostatic).

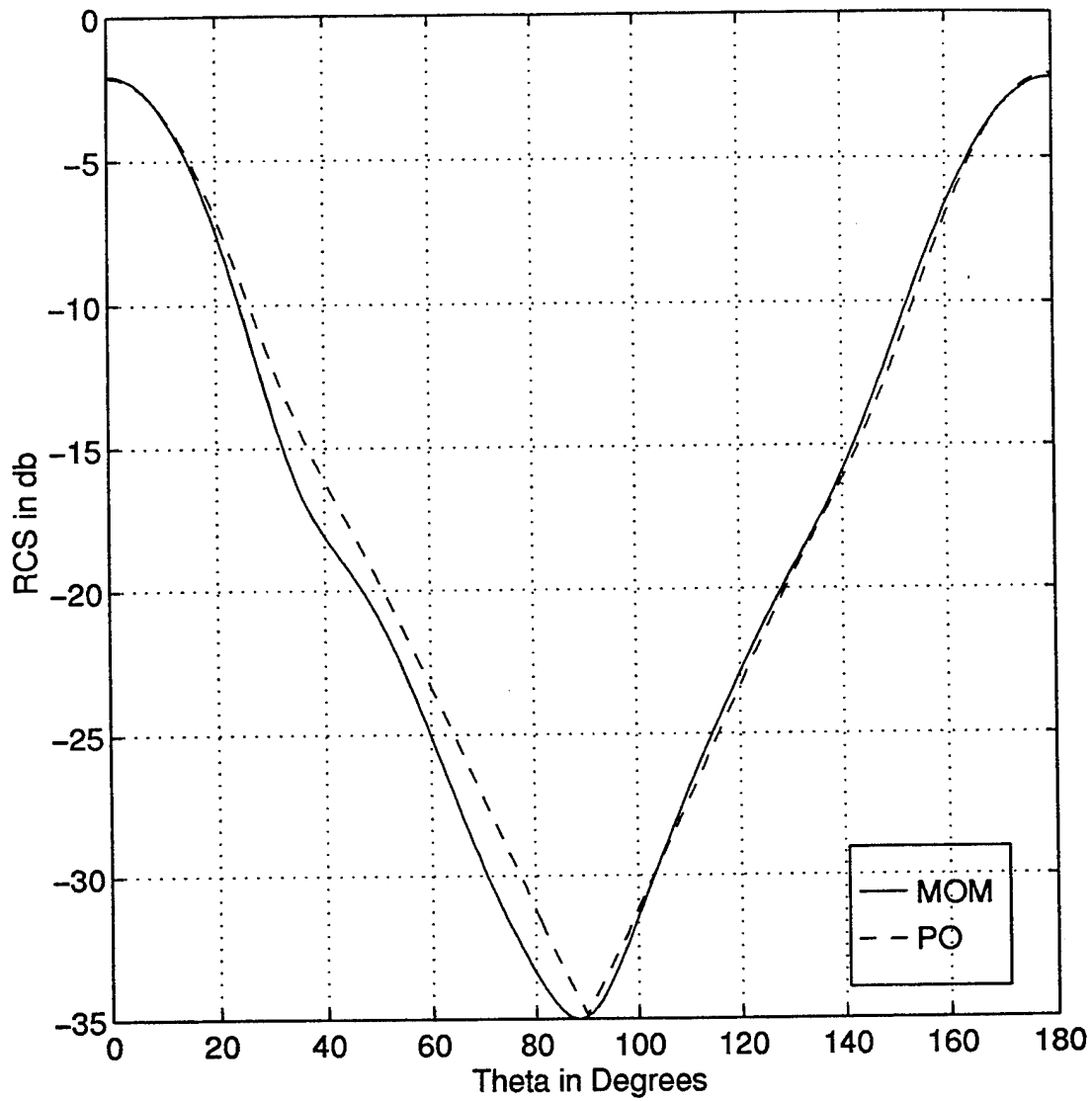


Figure 15. RCS for a spherical cap with  $377 \Omega/\square$  surface resistivity (TM polarized incident wave, monostatic).

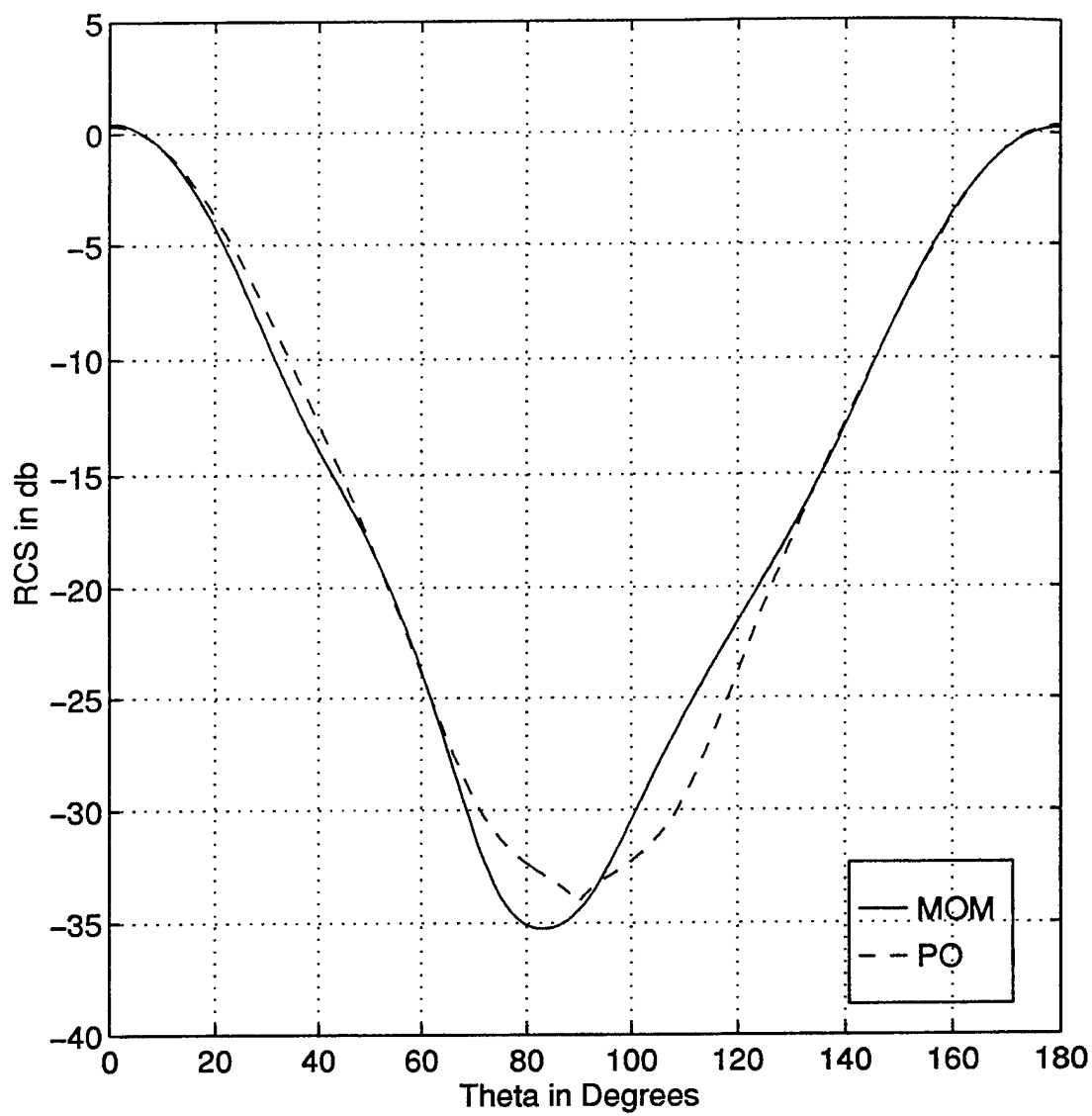


Figure 16. RCS of a spherical cap with surface resistivity given by equation (4.2) (TM polarized incident wave, monostatic).

## B. RCS SYNTHESIS

The synthesis computer code is similar to the program POTEEST with changes to utilize DCS samples rather than  $\phi$  and  $\theta$ . The increments  $du$  and  $dv$  were calculated so that  $N$  would equal the number of triangles on the surface of the object. A short program, NBOX, was used to insure this. After the number of boxes and triangles were matched, the program POTCO2 was used to calculate the field scattered from the object at the required  $u$  and  $v$  points. The scattered field was then used in SYNTH to calculate the resistance on each triangle based on the given field. Listings of all of these programs are included in the appendix.

First, a flat conducting plate was again used as a test case. For this calculation,  $N=80$ ,  $du=dv=0.2$ . The synthesized resistivity was expected to be  $0 \Omega/\square$  across all triangles, and this was indeed the result. Next, the plate was given a constant resistivity of  $377 \Omega/\square$ . The synthesized resistivity exactly matched the expected original values. Finally, the plate was given a linear resistivity across the triangles. The synthesized resistivity was within less than one percent of the expected result. A comparison plot of the original resistivity and the synthesized is shown in Figure 17 on the following page. Note that adjacent triangles have different midpoints and therefore the resistivity curve oscillates.

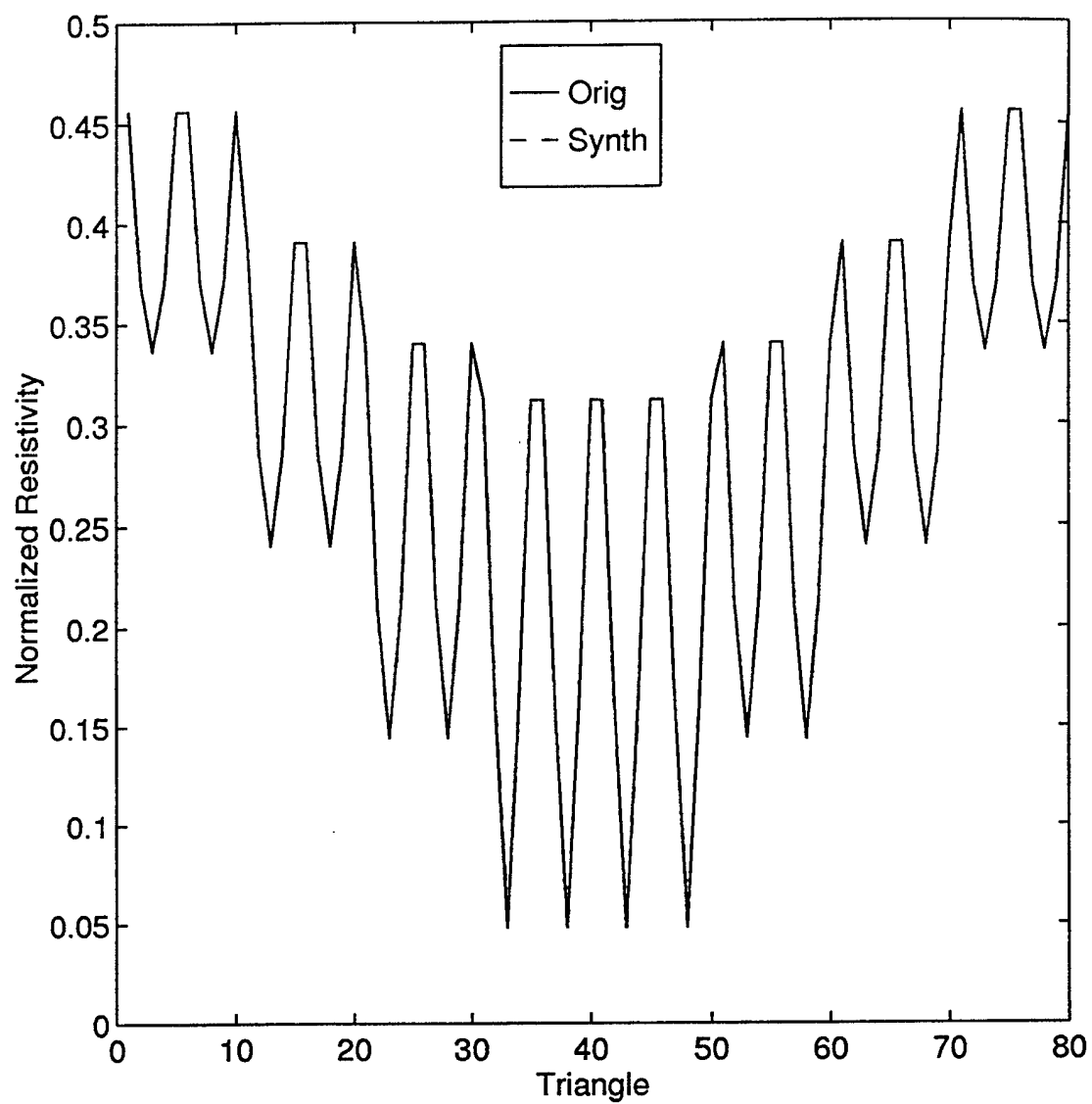


Figure 17. Original resistivity compared with synthesized resistivity (flat plate, surface resistivity given by equation (4.1)).

The flat disk was next used to calculate the synthesized resistivity. For this calculation,  $N=156$ ,  $du=dv=0.1429$ . With a constant resistivity of  $0 \Omega/\square$  and  $377 \Omega/\square$ , the synthesized resistivity was within one percent of the original value. This is shown in Figures 18 and 19 respectively. With a linear resistivity given by equation (4.1), the synthesized resistivity was exactly the same as the original resistivity, as shown in Figure 20.

Finally, resistivity synthesis was conducted for a spherical cap. For this calculation,  $N=156$ ,  $du=dv=0.1429$ . The synthesized resistivities for cases  $0 \Omega/\square$  and  $377 \Omega/\square$  were within one percent of the original resistivities. This is shown in Figures 21 and 22. The results for a linear resistivity given by equation (4.2) were exactly the same as the original values. This is shown in Figure 23.

In order to verify the synthesized resistivity would yield the correct RCS, a comparison was made between the original RCS and the synthesized RCS. For all three geometries,  $0 \Omega/\square$ ,  $377 \Omega/\square$ , and linear resistivity, the synthesized resistivities were used in the MOM code to compute the RCS patterns. The results are shown in Figures 24 through 32. The curves labeled Orig are the PO RCS values used to initiate the synthesis. Those labeled Synth were obtained using the synthesized resistivity in the MOM code, PATCH. These figures are essentially duplicates of Figures 8 through 16 because the synthesized resistivity was almost identical to the starting values.

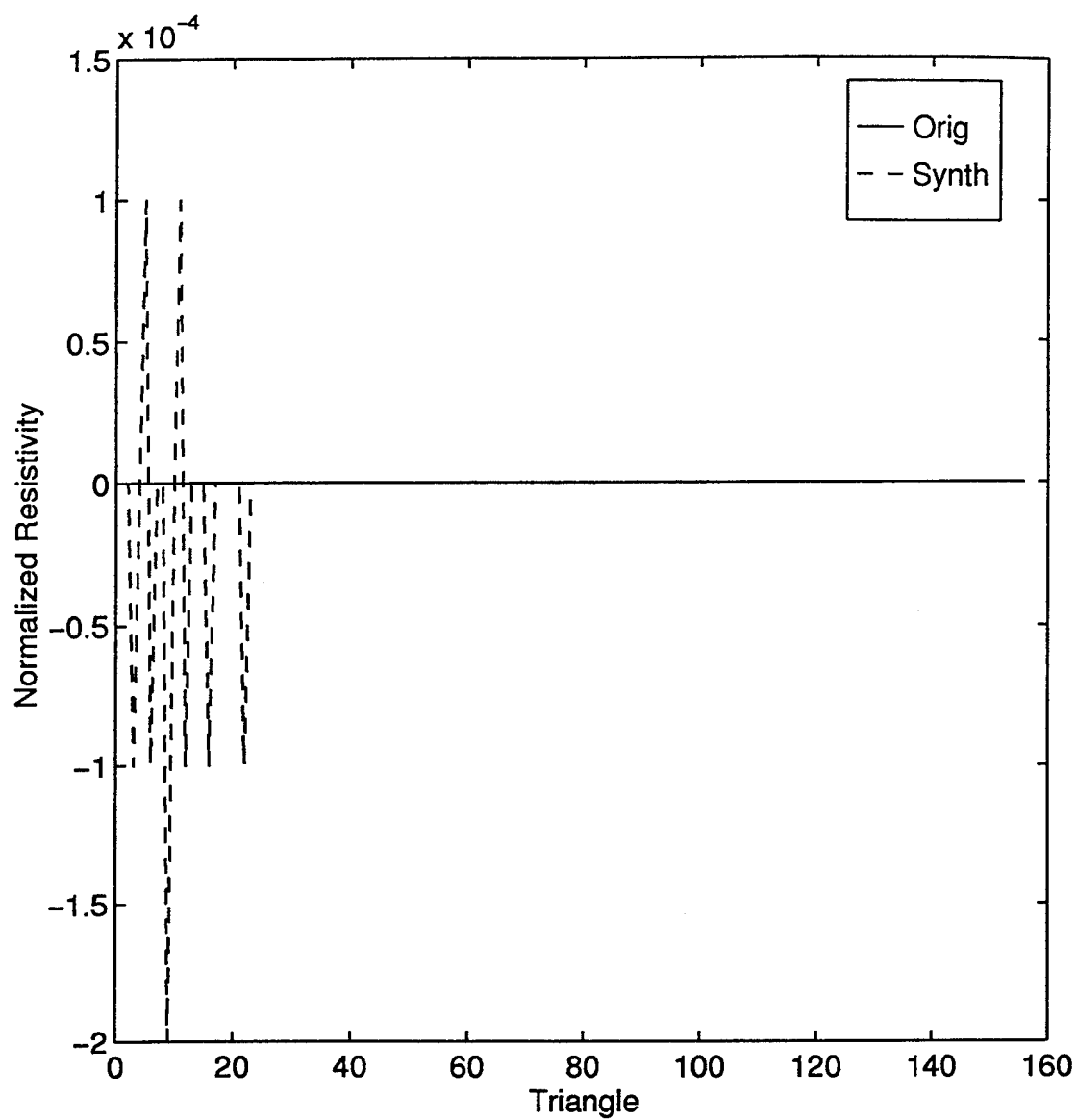


Figure 18. Original resistivity compared with synthesized resistivity (flat disk, 0  $\Omega/\square$  resistivity).

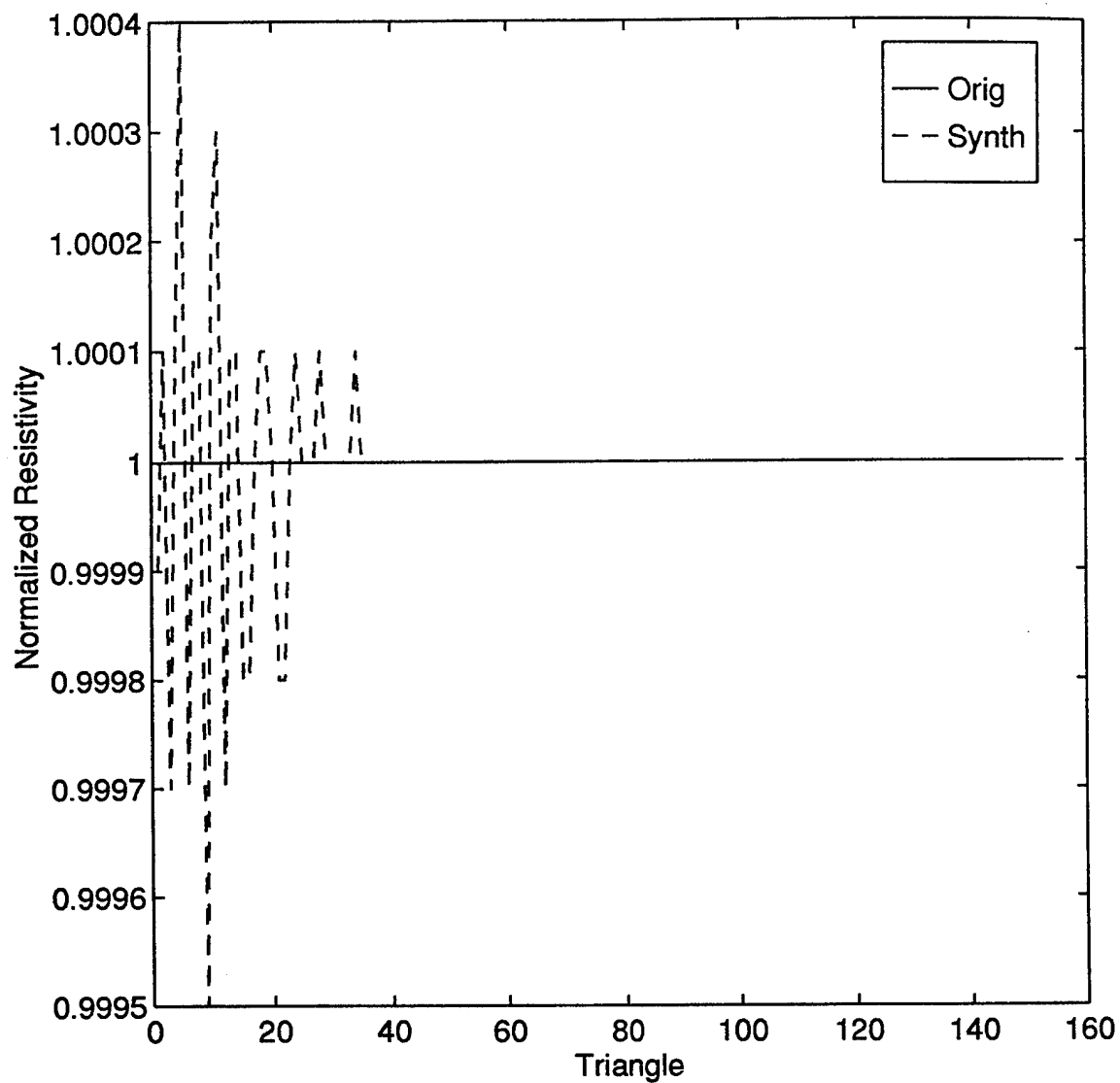


Figure 19. Original resistivity compared with synthesized resistivity (flat disk, 377  $\Omega/\square$  resistivity).

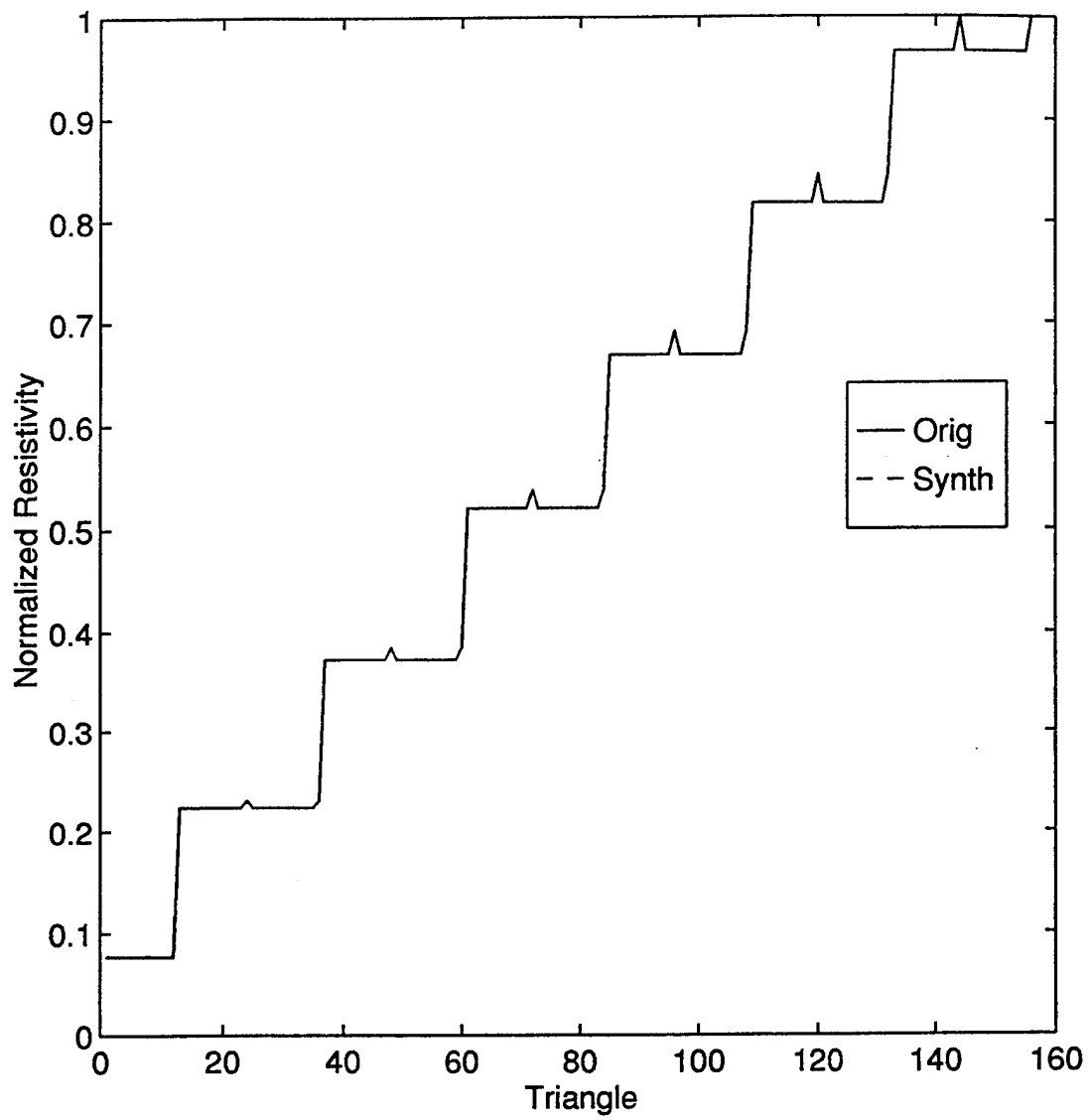


Figure 20. Original resistivity compared with synthesized resistivity (flat disk, surface resistivity given by equation (4.1)).

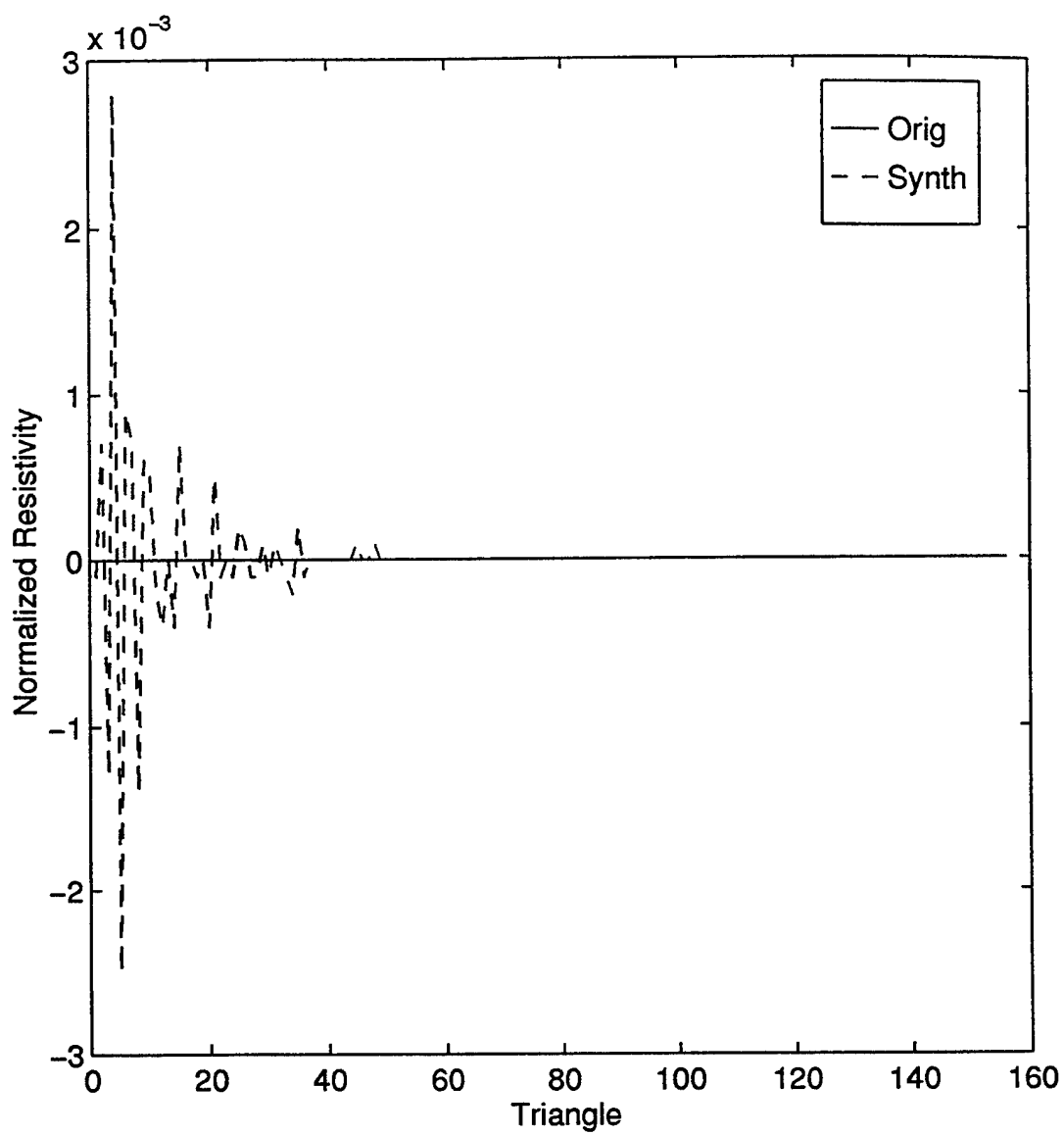


Figure 21. Original resistivity compared with synthesized resistivity (spherical cap, 0  $\Omega/\square$  resistivity).

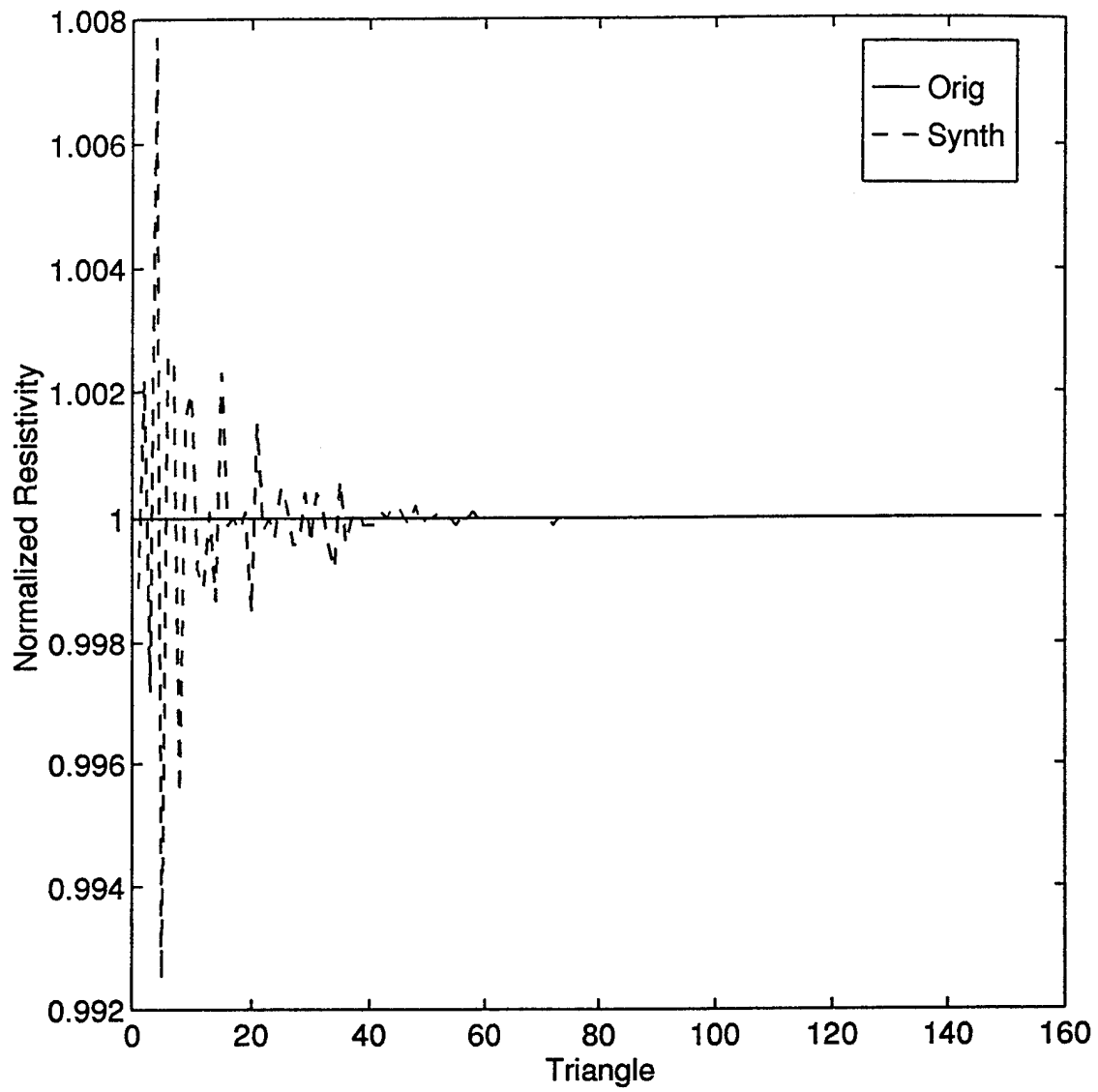


Figure 22. Original resistivity compared with synthesized resistivity (spherical cap, 377  $\Omega/\square$  resistivity).

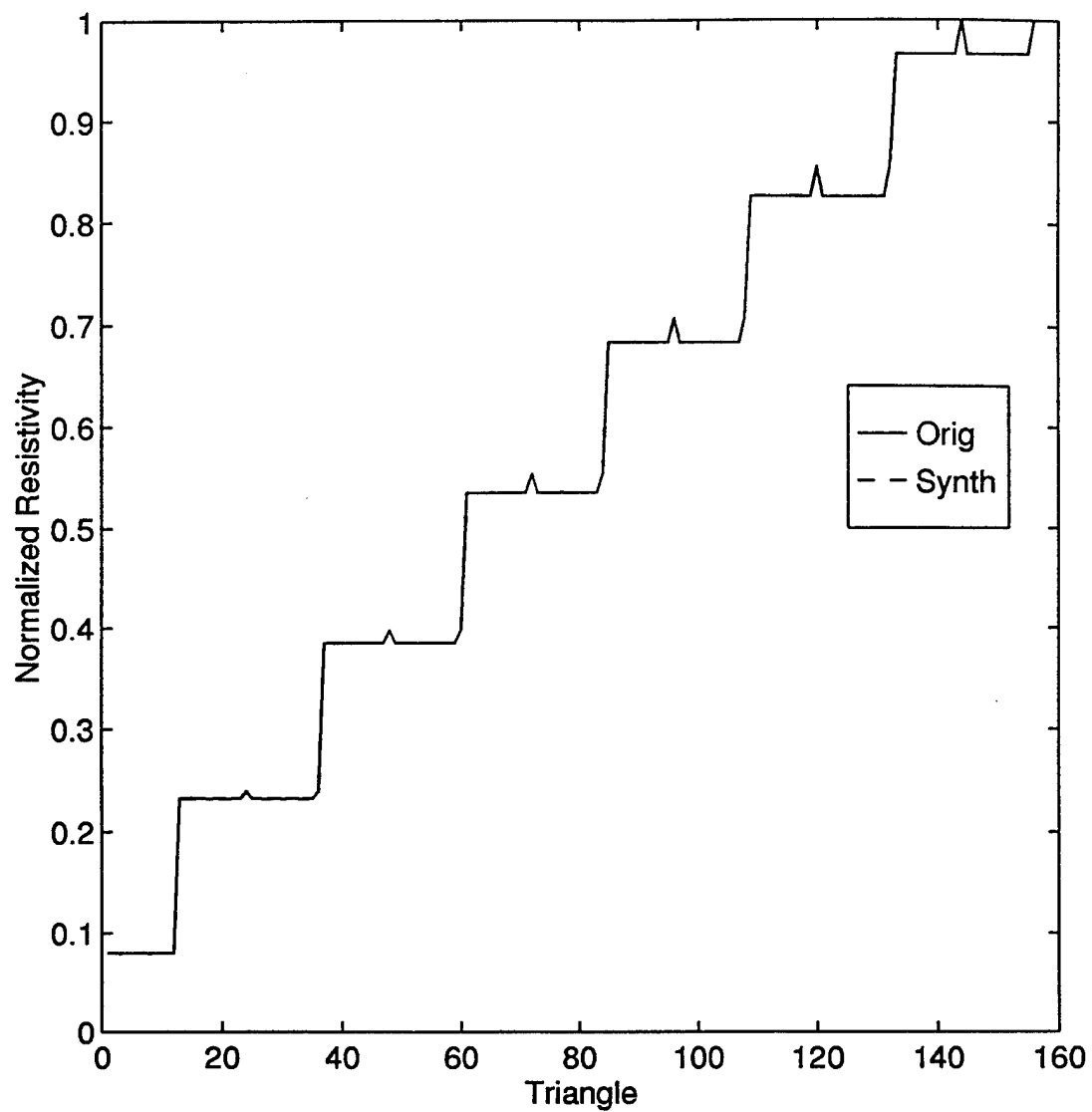


Figure 23. Original resistivity compared with synthesized resistivity (spherical cap, surface resistivity given by equation (4.2)).

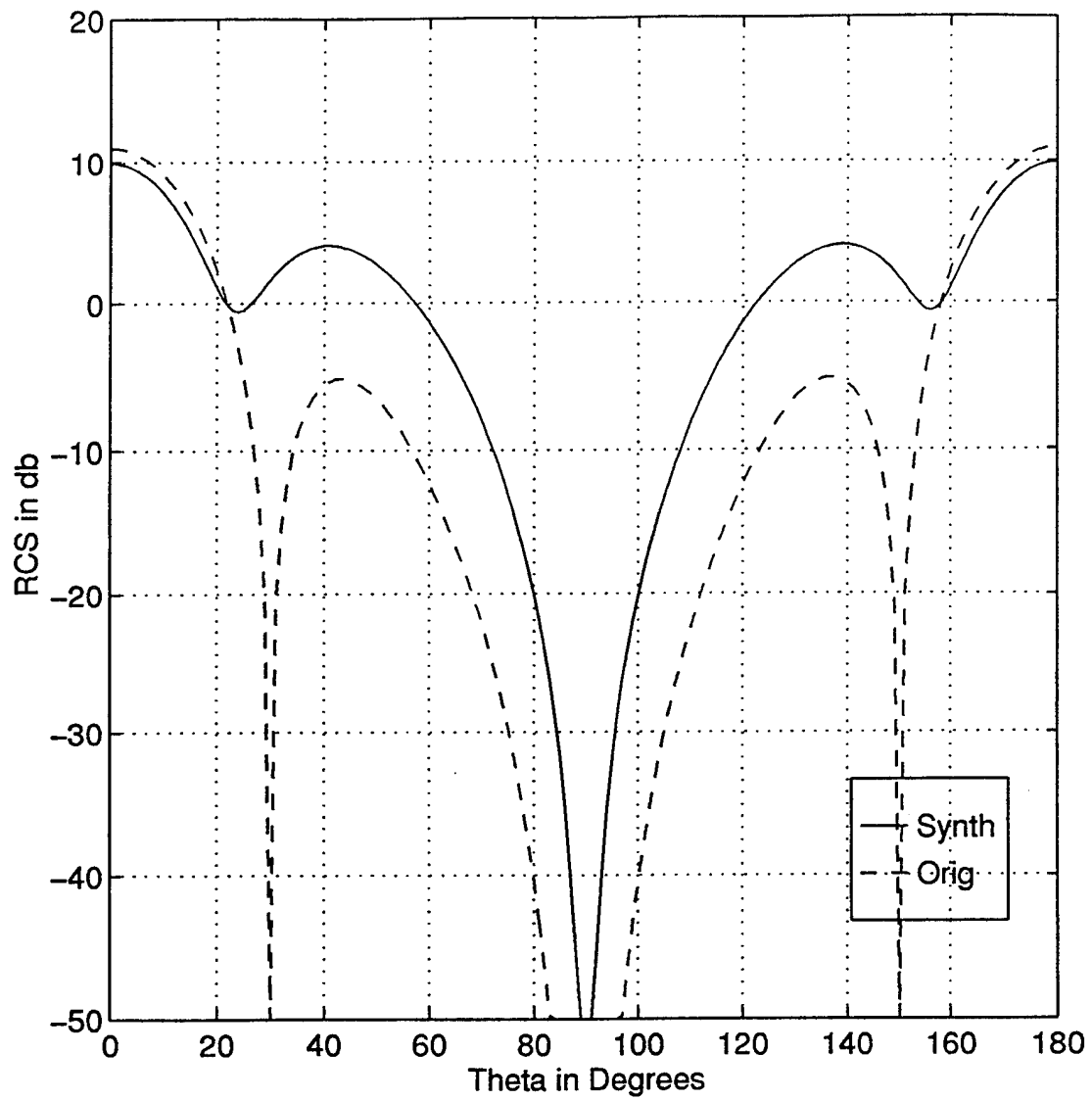


Figure 24. Original RCS compared with synthesized RCS (flat plate, 0  $\Omega/\square$  resistivity).

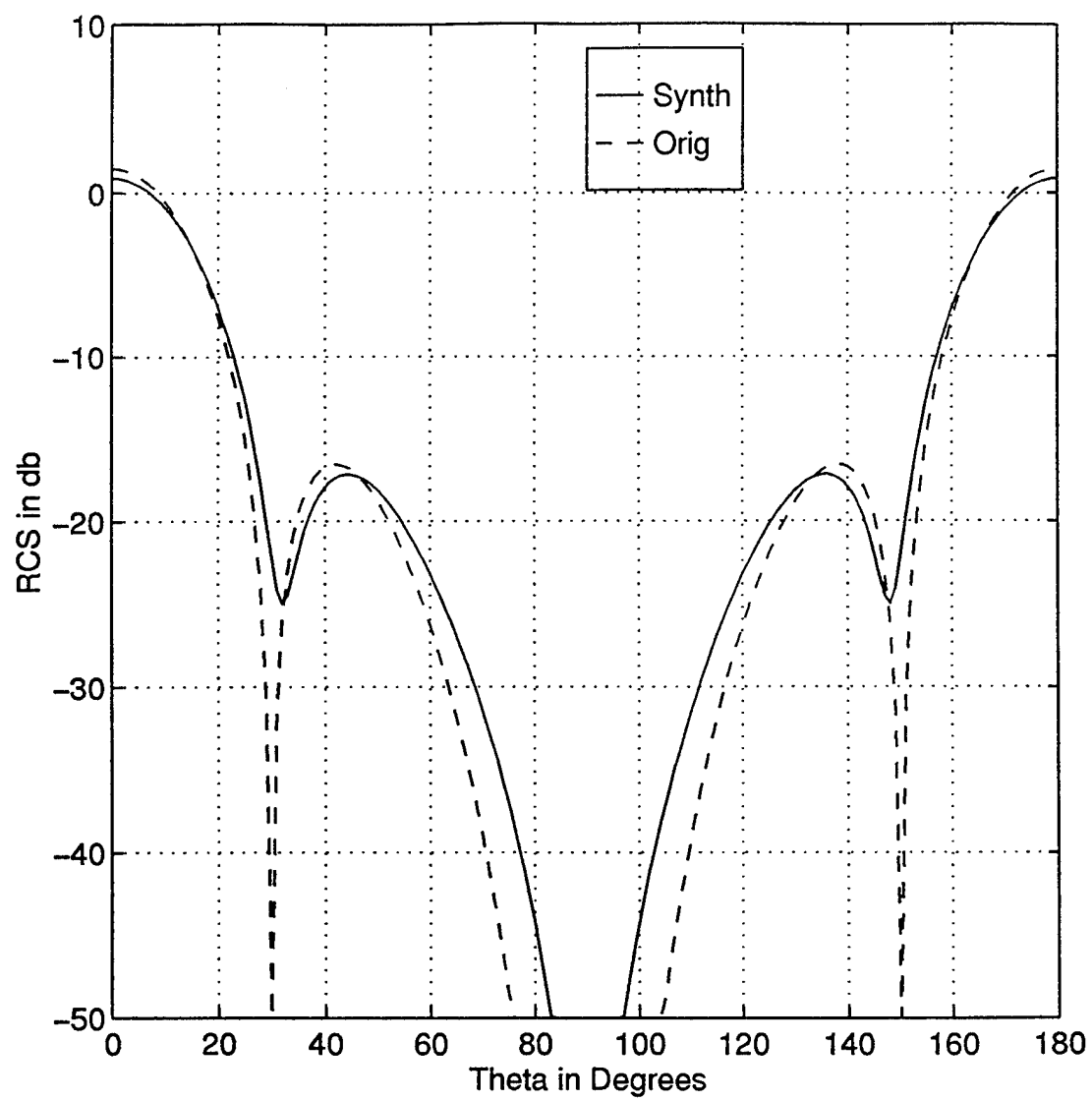


Figure 25. Original RCS compared with synthesized RCS (flat plate, 377  $\Omega/\square$  resistivity).

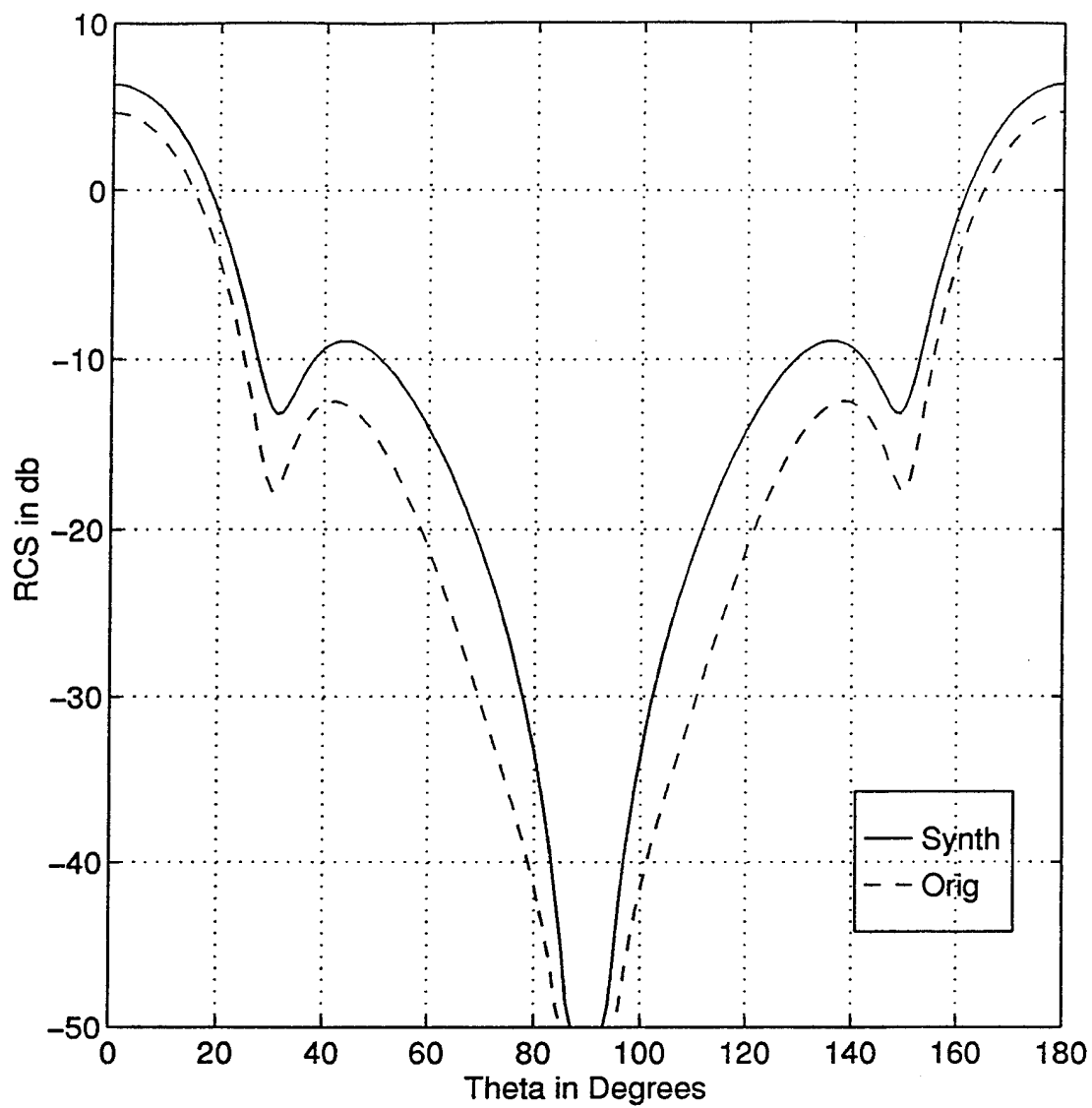


Figure 26. Original RCS compared with synthesized RCS (flat plate, surface resistivity given by equation (4.1)).

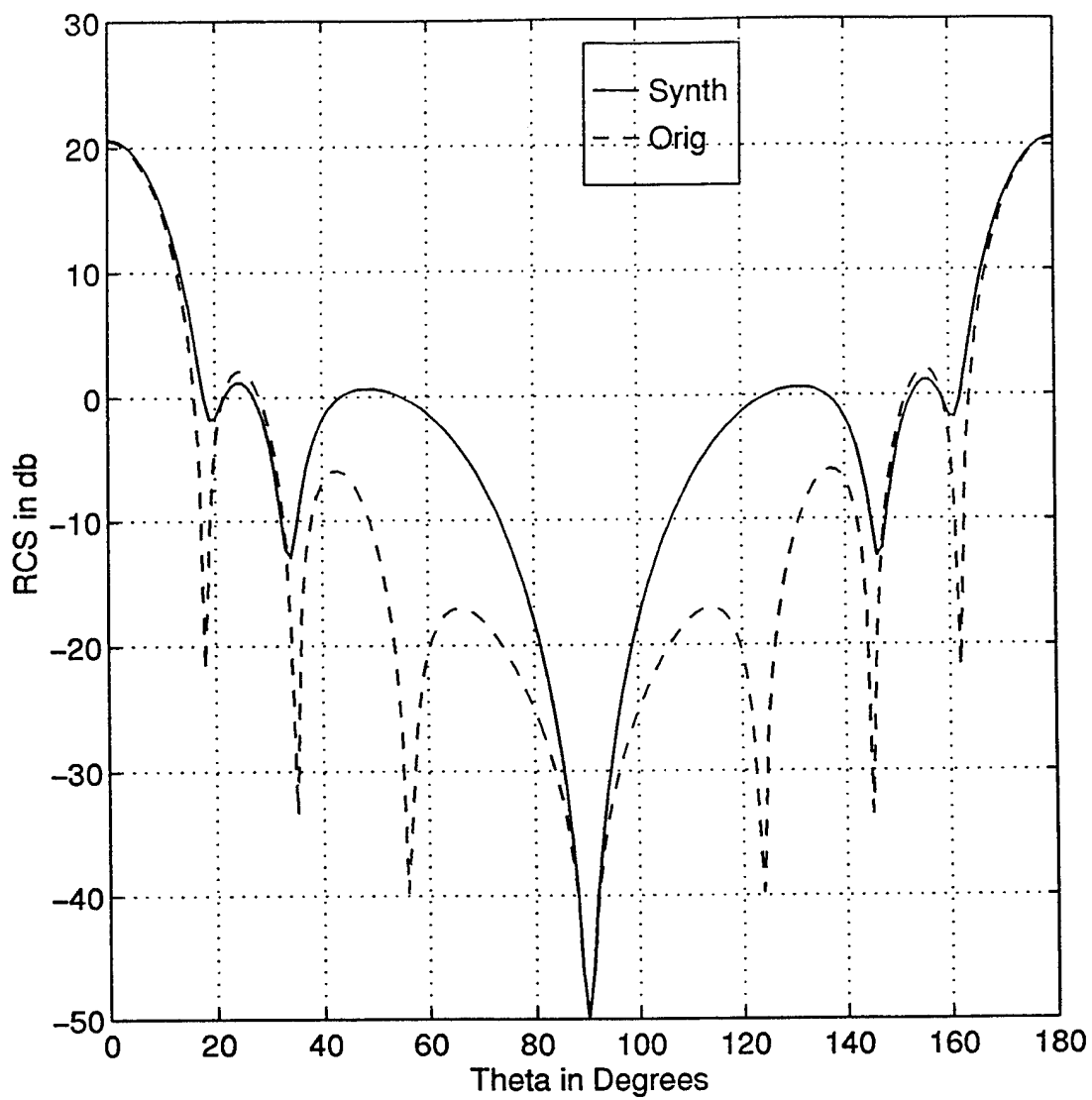


Figure 27. Original RCS compared with synthesized RCS (flat disk, 0  $\Omega/\square$  resistivity).

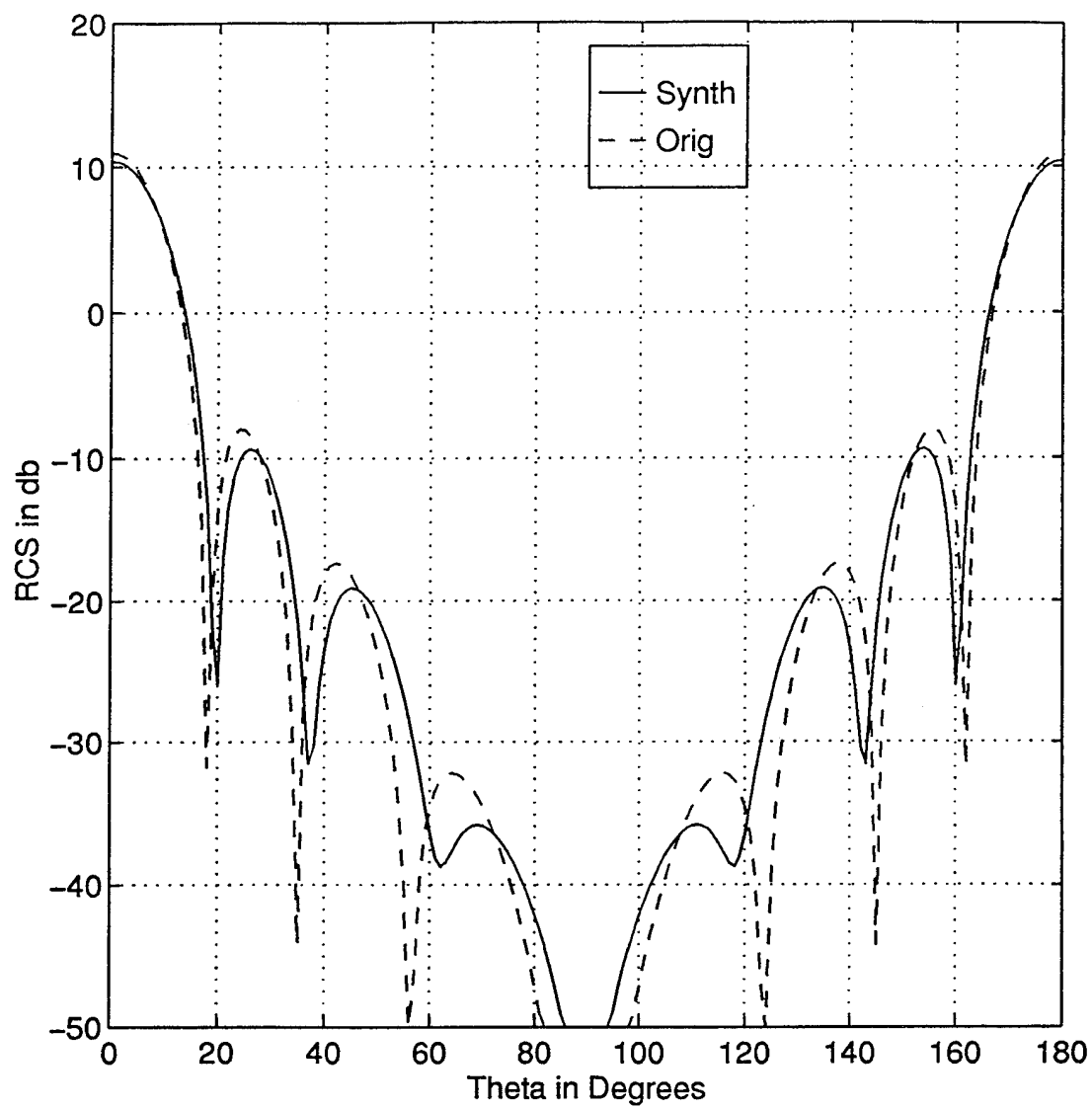


Figure 28. Original RCS compared with synthesized RCS (flat disk, 377  $\Omega/\square$  resistivity).

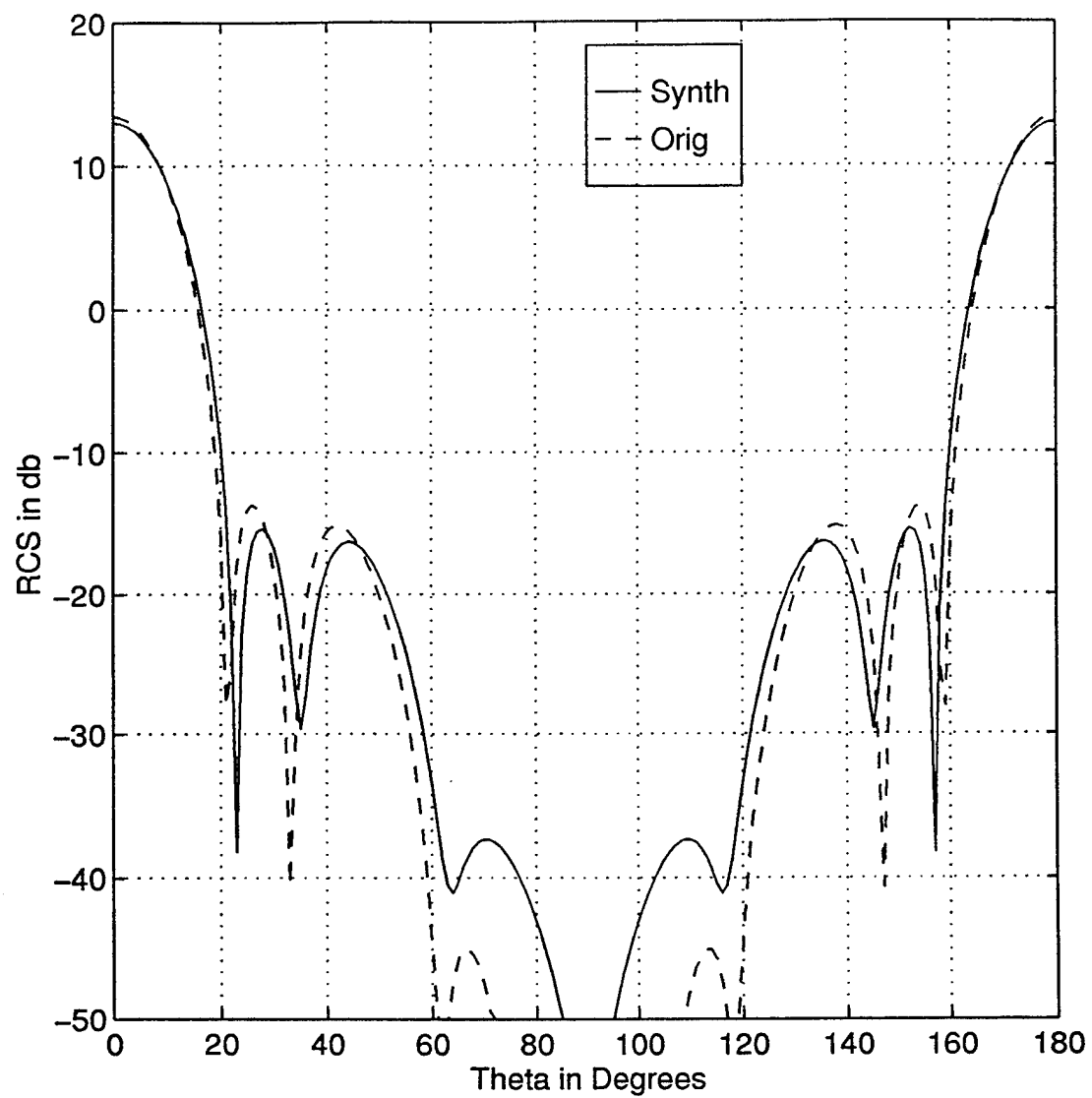


Figure 29. Original RCS compared with synthesized RCS (flat disk, surface resistivity given by equation (4.1)).

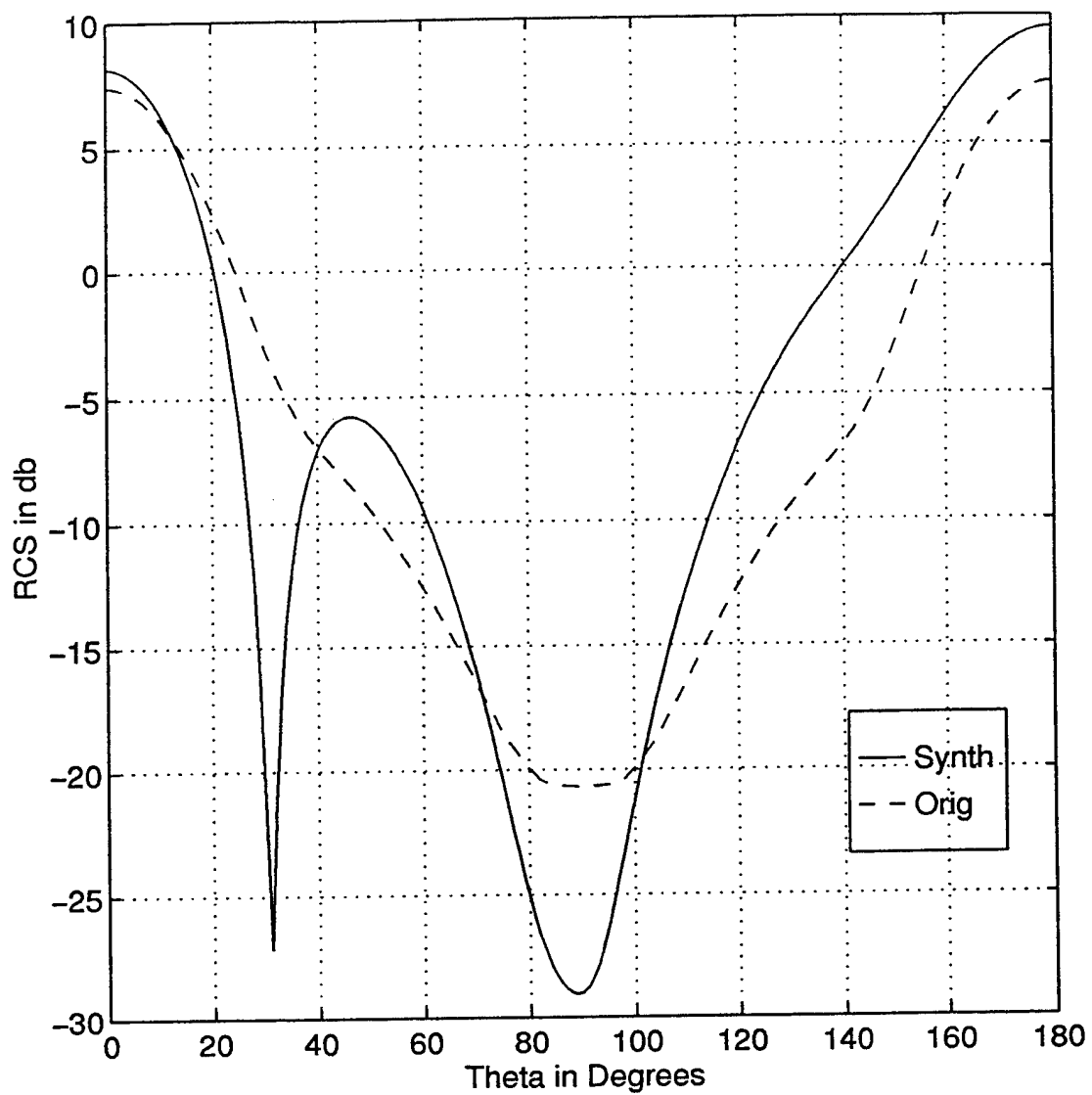


Figure 30. Original RCS compared with synthesized RCS (spherical cap, 0  $\Omega/\square$  resistivity).

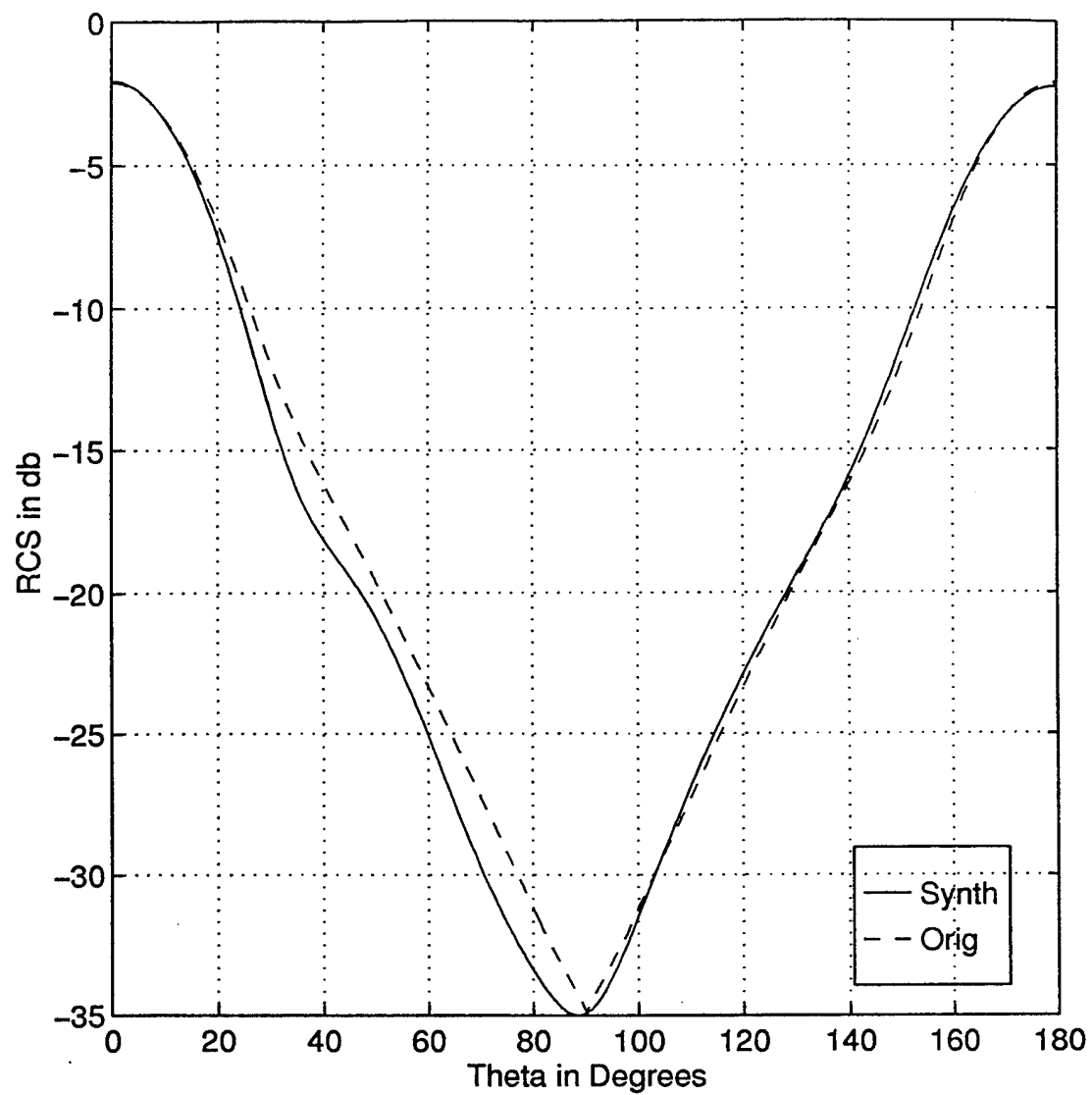


Figure 31. Original RCS compared with synthesized RCS (spherical cap, 377  $\Omega/\square$  resistivity).

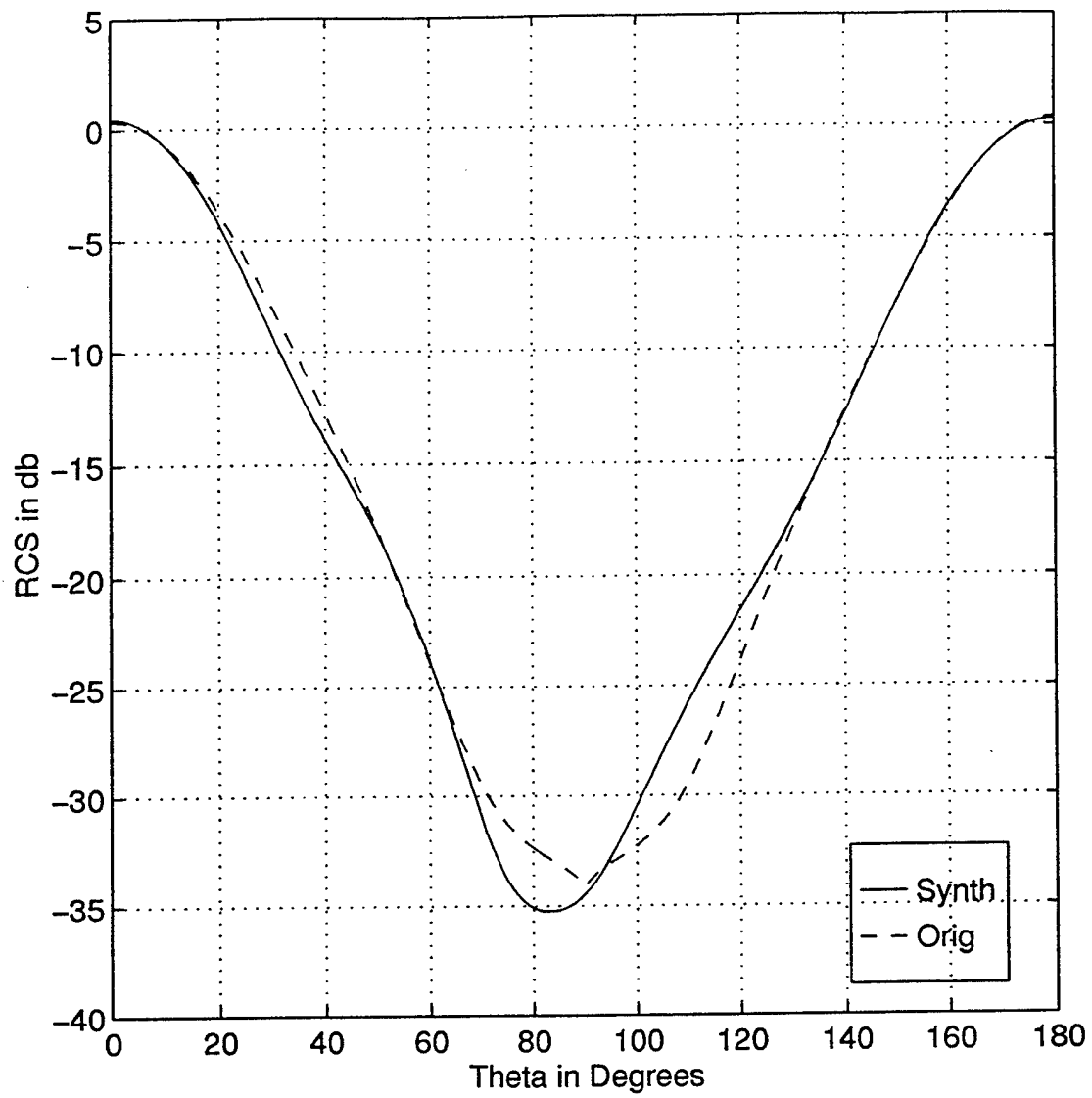


Figure 32. Original RCS compared with synthesized RCS (spherical cap, surface resistivity given by equation (4.2)).

## V. CONCLUSIONS

A procedure for synthesizing the RCS of a target of known shape has been presented. The equations were derived for both flat and doubly curved surfaces and demonstrated for monostatic, and purely resistive surfaces. The equations were derived using the physical optics approximation and, therefore, traveling waves were neglected. Furthermore, multiple reflections were neglected.

The RCS of each type of surface was first calculated using PO and then compared to MOM. Next, the RCS of each surface was calculated in DCS so the scattered field could be sampled and used in the synthesis equations. The synthesis equations were then used to find the resistivity across the surface. Finally, the resistivity obtained from the synthesis procedure was used to recalculate the RCS and, therefore, demonstrated that the synthesis procedure was accurate. The synthesized resistivities were in excellent agreement with the original values in spite of all of the approximations. This is because the chosen resistivity distributions yielded low RCS sidelobes and did not support traveling waves. Similarly, the resistive surface transmits more of the incident field than it reflects. Therefore, multiple reflections are not important and can usually be neglected in the synthesis of low RCS patterns.

A more rigorous solution could be obtained by using the MOM as the basis of the synthesis equations. [Ref. 3] This would require solving exactly for the current along the surface as well as for the resistivity. Future work in this area should include a synthesis procedure based on MOM.



## APPENDIX. COMPUTER CODES

This appendix contains all of the computer codes used for calculations in this thesis. The code PTEST.M calculates the RCS of a surface with specified resistivity. The code POTCO2.M calculates the RCS of a surface in DCS. The code BUILD.M generates the geometry of the surface. The code FACT.M is a subroutine used to calculate the factorial of a number and is used with PTEST.M and POTCO2.M. The code GF.M is a subroutine used to calculate equation (3.28) and is used with PTEST.M and POTCO2.M. The code RES.M is a subroutine used in the calculation of linear resistivity across a surface using equations (4.1) and (4.2) and is used with PTEST.M and POTCO2.M. The code SYNTH.M reconstructs the resistivity using the scattered field from POTCO2.M. The code NBOX.M calculates the number of partitions of DCS that are within the visible region for a given  $du(=dv)$ . This was used to verify that the number of known scattered field points would be equal to the number of triangular subsections on the surface. The code POS.M compares the original RCS with the synthesized RCS.

```

% PTEST.M
% PO scattering from triangles
clear all
% illumination flag: =0 external face only
iflag=1;
Lt=.001;
Nt=2;
wave=1;
bk=2*pi/wave;
rad=pi/180;
% Incident wave polarization
Et=1+j*0; %TM-z
Ep=0+j*0; %TE-z
phi=0;
phr=phi*rad;
cp=cos(phr);sp=sin(phr);
% Wave amplitude at all vertices
Co=1.;
build
ntria=nfaces;
nvert=nverts;
x=xpts;
y=ypts;
z=zpts;
title('triangular model of the scattering surface')
xlabel('x')
ylabel('y')
zlabel('z')
for i=1:nvert
    text(x(i)-max(x)/20,y(i)-max(x)/20,z(i),num2str(i))

```

```

end
hold off
disp('hit return to continue calculation')
pause

% Define position vectors to vertices
for i=1:nvert;
    r(i,:)=[x(i) y(i) z(i)];
end
%Use res.m program to calculate resistivity
res
% Get resistivity, edge vectors and normals from edge cross
products

for i=1:ntria
    rs(i)=0;
    % Resistivity function for a flat surface
    %rs(i)=rss*sqrt(xm(i)^2+ym(i)^2)/377;
    % Resistivity function for a doubly curved surface
    %rs(i)=rss*arc(i)/377;
    A=r(vind(i,2),:)-r(vind(i,1),:);
    B=r(vind(i,3),:)-r(vind(i,1),:);
    C=r(vind(i,3),:)-r(vind(i,2),:);
    N(i,:)=cross(A,B);
    % check for proper direction of normal vector
    if N(i,3)<0
        N(i,:)=-N(i,:);
    end
    % Edge lengths for triangle "i"
    d(i,1)=norm(A);

```

```

        d(i,2)=norm(B);
        d(i,3)=norm(C);
        ss=.5*sum(d(i,:));
        Area(i)=sqrt(ss*(ss-d(i,1))*(ss-d(i,2))*(ss-d(i,3)));
        Nn=norm(N(i,:));
        N(i,:)=N(i,+)/Nn;

%transform triangles into local coordinates
x1=[1 0 0];
y1=[0 1 0];
z1=[0 0 1];
end % end of triangle loop

% Pattern Loop
start=0;
stop=180;
del=1;
it=floor((stop-start)/del)+1;
for i=1:it
    theta(i)=start+(i-1)*del;
    thr=theta(i)*rad;
    st=sin(thr); ct=cos(thr);
    u=st*cp; v=st*sp; w=ct;
    up=ct*cp; vp=ct*sp; wp=-st;
% Spherical coordinate system unit vectors
    R(i,:)=[u v w];
% Change Efield into global rectangular coordinates
    strtra(1,:)=[st*cp ct*cp -sp];
    strtra(2,:)=[st*sp ct*sp cp];
    strtra(3,:)=[ct -st 0];

```

```

sei=[0 Et Ep];
ei=strtra*sei';
% correct orientation for normal after 90deg
if theta(i)==91
    N=-N;
end
% Begin loop over triangles
    sumt=0;
    sump=0;
for m=1:ntria
    t(m,:)=cross(z1,N(m,:));
    beta(m)=acos(N(m,3));
    alpha(m)=atan2(t(m,2),t(m,1)+1e-6)-pi/2;
    % Test to see if front face is illuminated
        ndotk=N(m,:)*R(i,:)';
        if ndotk >= 0 & iflag==0 | iflag~=0
%translation into local coordinates
%first rotate about z axis
    tra1(1,:)=[cos(alpha(m)) sin(alpha(m)) 0];
    tra1(2,:)=[-sin(alpha(m)) cos(alpha(m)) 0];
    tra1(3,:)=[0 0 1];
    % Rotation about yp axis
    tra2(1,:)=[cos(beta(m)) 0 -sin(beta(m))];
    tra2(2,:)=[0 1 0];
    tra2(3,:)=[ sin(beta(m)) 0 cos(beta(m))];
    D1=tra1*R(i,:)';
    D2=tra2*D1;
    upp=D2(1);
    vpp=D2(2);
    wpp=D2(3);

```

```

% Find spherical angles in local coordinates
stpp=sqrt(upp^2+vpp^2)*sign(wpp);
ctpp=sqrt(1-stpp^2);
thpp=acos(ctpp);
phipp=atan2(vpp,upp+1e-10);
% Phase at the vertices of triangle m; monostatic RCS needs
"2"
    Dp=2*bk*((x(vind(m,1))-x(vind(m,3)))*u+...

(y(vind(m,1))-y(vind(m,3)))*v+...

(z(vind(m,1))-z(vind(m,3)))*w);
    Dq=2*bk*((x(vind(m,2))-x(vind(m,3)))*u+...

(y(vind(m,2))-y(vind(m,3)))*v+...

(z(vind(m,2))-z(vind(m,3)))*w);
    Do=2*bk*(x(vind(m,3))*u+y(vind(m,3))*v+z(vind(m,3))*w);
%incident field in local rectangular coordinates
eip=tra1*ei;
eipp=tra2*eip;
% translation of E-field into local spherical coordinates
strtra2=[stpp*cos(phipp)    ctp*cos(phipp)    -sin(phipp);
stpp*sin(phipp) ctp*sin(phipp) cos(phipp); ctp -stpp 0];
epp=strtra2^(-1)*eipp;
%Reflection coefficients
gamp=0;
    if (2*rs(m)+ctpp)~=0
        gamp=1/(2*rs(m)+ctpp);
    end

```

```

gamn=1/(2*rs(m)*cos(thpp)+1);
%Surface Currents
Jxpp(i,m)=(epp(2)*gamp-epp(3)*gamn)*ctpp^2;
Jypp(i,m)=(epp(2)*gamp+epp(3)*gamn)*ctpp;
% Area integral for general case
DD=Dq-Dp;
expDo=exp(j*Do);
expDp=exp(j*Dp);
expDq=exp(j*Dq);
% Special Case 1
if abs(Dp) < Lt & abs(Dq) >= Lt
    sic=0.;
    for n=0:Nt

sic=sic+(j*Dp)^n/fact(n)*(-Co/(n+1)+expDq*(Co*gf(n,-Dq)));
        end
        Ic(i,m)=sic*2*Area(m)*expDo/j/Dq;
% Special Case 2
        elseif abs(Dp) < Lt & abs(Dq) < Lt
            sic=0.;
            for n=0:Nt

                                for nn=0:Nt

sic=sic+(j*Dp)^n*(j*Dq)^nn/fact(nn+n+2)*Co;
                                end
                            end
                            Ic(i,m)=sic*2*Area(m)*expDo;
% Special Case 3

            elseif abs(Dp) >= Lt & abs(Dq) < Lt

```

```

        sic=0.;
        for n=0:Nt

sic=sic+(j*Dq)^n/fact(n)*Co*gf(n+1,-Dp)/(n+1);
            end
            Ic(i,m)=sic*2*Area(m)*expDo*expDp;
% Special Case 4
            elseif abs(Dp) >= Lt & abs(Dq) >= Lt & abs(DD) < Lt
                sic=0.;
                for n=0:Nt
                    sic = sic+(j*DD)^n/fact(n)*(-Co*gf(n,Dq)+expDq*Co/(n+1));
                end
                Ic(i,m)=sic*2*Area(m)*expDo/j/Dq;
            else

Ic(i,m)=2*Area(m)*expDo*(expDp*Co/Dp/DD-expDq*Co/Dq/DD-Co/Dp
/Dq);

                end                                % end of special cases
test
%Scattered field in local rectangular coordinates
Esxpp=Jxpp(i,m)*Ic(i,m);
Esypp=Jypp(i,m)*Ic(i,m);
Eszpp=0;
%retranslation to global rectangular coordinates
Esp(m,:)=[Esxpp Esypp Eszpp];
Es1=tra2^(-1)*Esp(m,:);
Es=tra1^(-1)*Es1;
%retranslation to global spherical coordinates
%seipp(m,:)=strtra^(-1)*Es;
seipp(m,1)=0;

```

```

seipp(m,2)=ct*cp*Es(1)+ct*sp*Es(2)-st*Es(3);
seipp(m,3)=-sp*Es(1)+cp*Es(2);
%sum over all triangles to get scattered field
sumt=sumt+seipp(m,2);
sump=sump+seipp(m,3);

end %end of illumination test
end %end of triangle loop
Eth=sumt;
Sth(i)=10*log10(4*pi*abs(Eth)^2+1.e-10);
Eph=sump;
Sph(i)=10*log10(4*pi*abs(Eph)^2+1.e-10);
end
Sth(:)=max(Sth(:),-50);
Sph(:)=max(Sph(:),-50);
%plot rcs
figure(2)
plot(theta,Sth,theta,Sph,'--'),grid
title('solid: co-polarization    dashed: cross-polarization')
xlabel('monostatic angle, theta (deg)')
ylabel('sigma/wav1^2 (dB)')

```

```

% POTCO2.M
% PO scattering from triangles
clear all
format long
% illumination flag: =0 external face only
iflag=0;
Lt=.001;
Nt=2;
wave=1;
bk=2*pi/wave;
rad=pi/180;
% Incident wave polarization
Et=1+j*0; %TM-z
Ep=0+j*0; %TE-z
% Wave amplitude at all vertices
Co=1.;
build
ntria=nfaces;
nvert=nverts;
x=xpts;
y=ypts;
z=zpts;
title('triangular model of the scattering surface')
xlabel('x')
ylabel('y')
zlabel('z')
for i=1:nvert
    text(x(i)-max(x)/20,y(i)-max(x)/20,z(i),num2str(i))
end
hold off

```

```

disp('hit return to continue calculation')
pause
% Define position vectors to vertices
for i=1:nvert;
    r(i,:)=[x(i) y(i) z(i)];
end
%Use res.m program to calculate resistivity
%res
% Get resistivity, edge vectors and normals from edge cross
products
for i=1:ntria
    rs(i)=0;
    %resistivity for a plate
    %rs(i)=rss*sqrt((xm(i)-.5)^2+(ym(i)-.5)^2)/377;
    % resistivity for a disk
    %rs(i)=rss*sqrt(xm(i)^2+ym(i)^2)/377;
    % resistivity for a cap
    %rs(i)=rss*arc(i)/377;
    ac(i)=1/(2*rs(i)+1);
    A=r(vind(i,2),:)-r(vind(i,1),:);
    B=r(vind(i,3),:)-r(vind(i,1),:);
    C=r(vind(i,3),:)-r(vind(i,2),:);
    N(i,:)=cross(A,B);
    % check for proper direction of normal vector
    if N(i,3)<0
        N(i,:)=-N(i,:);
    end
    % Edge lengths for triangle "i"
    d(i,1)=norm(A);
    d(i,2)=norm(B);

```

```

    d(i,3)=norm(C);
    ss=.5*sum(d(i,:));
    Area(i)=sqrt(ss*(ss-d(i,1))*(ss-d(i,2))*(ss-d(i,3)));
    Nn=norm(N(i,:));
    N(i,:)=N(i,:)/Nn;
%transform triangles into local coordinates
x1=[1 0 0];
y1=[0 1 0];
z1=[0 0 1];
end
% Pattern Loop
it=0;
load du.m;
k=0;
for u1=-1:du:1-du
    for v1=-1:du:1-du;
        it=it+1;

    Eth(it)=0;
    Eph(it)=0;
%test to see if center of box is within visible region
    test=((u1+du/2)^2+(v1+du/2)^2);
    if test<=1
        k=k+1;
        phi=atan2((v1+du/2),(u1+du/2));
        cp=cos(phi); sp=sin(phi);
        theta=asin(sqrt(test));
        st=sin(theta); ct=cos(theta);
% Center of box is used so u and v are redefined using center
of % box
        u=st*cp; v=st*sp; w=ct;
    end
end

```

```

        up=ct*cp; vp=ct*sp; wp=-st;
% Spherical coordinate system unit vectors
        R(it,:)= [u v w];
% Change Efield into global rectangular coordinates
        strtra(1,:)= [st*cp ct*cp -sp];
        strtra(2,:)= [st*sp ct*sp cp];
        strtra(3,:)= [ct -st 0];
        sei=[0 Et Ep];
        ei=strtra*sei';
% Begin loop over triangles
        for m=1:ntria
            t(m,:)=cross(z1,N(m,:));
            beta(m)=acos(N(m,3));
            alpha(m)=atan2(t(m,2),t(m,1)+1e-6)-pi/2;
            Ic(k,m)=0;
% Test to see if front face is illuminated
            ndotk=N(m,:)*R(it,:);
            if ndotk >= 0 & iflag==0 | iflag~=0
%translation into local coordinates
%first rotate about z axis
            tra1(1,:)= [cos(alpha(m)) sin(alpha(m)) 0];
            tra1(2,:)= [-sin(alpha(m)) cos(alpha(m)) 0];
            tra1(3,:)= [0 0 1];
% Rotation about yp axis
            tra2(1,:)= [cos(beta(m)) 0 -sin(beta(m))];
            tra2(2,:)= [0 1 0];
            tra2(3,:)= [sin(beta(m)) 0 cos(beta(m))];
            D1=tra1*R(it,:);
            D2=tra2*D1;
            upp=D2(1);

```

```

vpp=D2(2);
wpp=D2(3);
% Find spherical angles in local coordinates
stpp=sqrt(upp^2+vpp^2)*sign(wpp);
ctpp=sqrt(1-stpp^2);
thpp=acos(ctpp);
phipp=atan2(vpp,upp+1e-10);
% Phase at the three vertices of triangle m; monostatic RCS
needs % "2"
    Dp=2*bk*((x(vind(m,1))-x(vind(m,3)))*u+...

(y(vind(m,1))-y(vind(m,3)))*v+...

(z(vind(m,1))-z(vind(m,3)))*w);
    Dq=2*bk*((x(vind(m,2))-x(vind(m,3)))*u+...

(y(vind(m,2))-y(vind(m,3)))*v+...

(z(vind(m,2))-z(vind(m,3)))*w);
    Do=2*bk*(x(vind(m,3))*u+y(vind(m,3))*v+z(vind(m,3))*w);

%incident field in local rectangular coordinates
eip=tral*ei;
eipp=tra2*eip;
% translation of E-field into local spherical coordinates
strtra2=[stpp*cos(phipp)    ctp*cos(phipp)    -sin(phipp);
stpp*sin(phipp) ctp*sin(phipp) cos(phipp); ctp -stpp 0];
epp=strtra2^(-1)*eipp;
% Area integral for general case
DD=Dq-Dp;

```

```

expDo=exp(j*Do);
expDp=exp(j*Dp);
expDq=exp(j*Dq);
% Special Case 1
if abs(Dp) < Lt & abs(Dq) >= Lt
    sic=0.;
    for n=0:Nt

sic=sic+(j*Dp)^n/fact(n)*(-Co/(n+1)+expDq*(Co*gf(n,-Dq)));
        end
        Ic(k,m)=sic*2*Area(m)*expDo/j/Dq;
% Special Case 2
        elseif abs(Dp) < Lt & abs(Dq) < Lt
            sic=0.;
            for n=0:Nt

                                                for nn=0:Nt

sic=sic+(j*Dp)^n*(j*Dq)^nn/fact(nn+n+2)*Co;
                                                end

            end
            Ic(k,m)=sic*2*Area(m)*expDo;
% Special Case 3
            elseif abs(Dp) >= Lt & abs(Dq) < Lt
                sic=0.;
                for n=0:Nt

sic=sic+(j*Dq)^n/fact(n)*Co*gf(n+1,-Dp)/(n+1);
                    end
                    Ic(k,m)=sic*2*Area(m)*expDo*expDp;
% Special Case 4

```

```

elseif abs(Dp) >= Lt & abs(Dq) >= Lt & abs(DD) < Lt
    sic=0.;
    for n=0:Nt
        s      i      c      =
        sic+(j*DD)^n/fact(n)*(-Co*gf(n,Dq)+expDq*Co/(n+1));
    end
    Ic(k,m)=sic*2*Area(m)*expDo/j/Dq;
    else
    Ic(k,m)=2*Area(m)*expDo*(expDp*Co/Dp/DD-expDq*Co/Dq/DD-Co/Dp
/Dq);
    end
% end of special cases test
end %end of illumination test
end %end of triangle loop
%sum over all triangles to get scattered field
Eth(it)=Ic(k,:)*ac'*Et;
Eph(it)=Ic(k,:)*ac'*Ep;
% correction for rounding errors
%Eth2(it)=round(Eth(it)*1e4);
%Eth(it)=Eth2(it)*1e-4;
end % end of test for visible region
Sth(it)=10*log10(4*pi*abs(Eth(it)/(Et+1e-10))^2+1.e-10);
Sph(it)=10*log10(4*pi*abs(Eph(it)/(Ep+1.e-10))^2+1.e-10);
end % end of v loop
end % end of u loop
Sth(:)=max(Sth(:),-50);
Sph(:)=max(Sph(:),-50);
Sth=Sth';
Sph=Sph';
%plot rcs

```

```

u=-1:du:1-du;
v=-1:du:1-du;
T=ones(1,2/du);
nrow=2/du;
ncol=2/du;
for k=1:ncol;
    k1=nrow*(k-1)+1;
    k2=k1+nrow-1;
    X2(:,k)=(u(k)+du/2)*T';
    Y2(:,k)=(du/2.+v)';
    Z2(:,k)=Sth(k1:k2);
end
figure(2)
orient tall
surf(X2,Y2,Z2)
view(-25,55)
colormap(hot)
xlabel('u')
ylabel('v')
zlabel('RCS in Db')
Eth=Eth';
Eph=Eph';
rs=rs';
Ethr=real(Eth);
Ethi=imag(Eth);
Ephr=real(Eph);
Ephi=imag(Eph);
Ici=imag(Ic);
save Ethr.m Ethr -ascii -double
save Ethi.m Ethi -ascii -double

```

```
save Ephr.m Ephr -ascii  
save Ephi.m Ephi -ascii  
save rs.m rs -ascii  
save Icr.m Ic -ascii  
save Ici.m Ici -ascii
```

```

% BUILD.M
% Program to read transposed "buildn5" data and plot it in
MATLAB
% node (x,y,z) coordinates
% legend:
load xpts.m
load ypts.m
load zpts.m
nverts=length(xpts);
% node connection list
load end1.m
load end2.m
nedges=length(end1);
% face connection list
load node1.m
load node2.m
load node3.m
nfaces=length(node3);
% load vind array which gives the three nodes for each
triangle
for i=1:nfaces
    pts=[node1(i) node2(i) node3(i)];
    vind(i,:)=pts;
end
figure(1)
% This section plots a mesh
if icur==0
    for i=1:nfaces
        X=[xpts(vind(i,1)) xpts(vind(i,2)) xpts(vind(i,3))
xpts(vind(i,1))];

```

```

        Y=[ypts(vind(i,1))  ypts(vind(i,2))  ypts(vind(i,3))
ypts(vind(i,1))];
        Z=[zpts(vind(i,1))  zpts(vind(i,2))  zpts(vind(i,3))
zpts(vind(i,1))];
        plot3(X,Y,Z,'m')
        if i == 1
            axis equal
            view(60,45)
            hold on
        end
    end
end
hold off

```

```
% FACT.M
% Subroutine for calculating the factorial of a number

function f=fact(m)
f=1;
if m>=1
    for n=1:m
        f=f*n;
    end
end
```

```

% GF.M
function gf=gf(n,w)
    gf=(exp(j*w)-1)/(j*w);
    if n>=0
        for m=1:n
            gf=(exp(j*w)-n*gf)/(j*w);
        end
    end
end

```

```

% RES.M
% Program to Calculate Resistivity on Each Triangle using a
% Linear Taper
for n=1:nfaces
    xm(n)=(r(max(vind(n,:)),1)+r(min(vind(n,:)),1))/2;
    ym(n)=(r(max(vind(n,:)),2)+r(min(vind(n,:)),2))/2;
    zm(n)=(r(max(vind(n,:)),3)+r(min(vind(n,:)),3))/2;
% vector to midpoint of each triangle
mn(n,:)=[xm(n) ym(n) zm(n)];
% angle from z axis to midpoint vector
if zm(n)~=0
    omega(n)=pi/2-acos(zm(n)/(sqrt(xm(n)^2+ym(n)^2)+1e-8));
%arclength from z axis to midpoint of each triangle
    arc(n)=xm(n)^2+ym(n)^2;
end
%arclength from z axis to midpoint if plate is not flat
    arc(n)=omega(n)/(2*pi);
end % end of triangle loop
rss=377/max(abs(arc));
end

```

```

% SYNTH.M
% Resistivity Synthesis-Monostatic
clear all
format long
% illumination flag: =0 external face only
iflag=0;
Lt=.001;
Nt=2;
wave=1;
bk=2*pi/wave;
rad=pi/180;
% Incident wave polarization
Et=1+j*0; %TM-z
Ep=0+j*0; %TE-z
% Load results from potcos program
load Ethr.m;
load Ethl.m;
Ethii=Ethl*i;
Eth=Ethr+Ethii;
load Ephr.m;
load Ephl.m;
Ephii=Ephl*i;
Eph=Ephr+Ephii;
load rs.m;
% Wave amplitude at all vertices
Co=1.;
build
ntria=nfaces;
nvert=nverts;
x=xpts;

```

```

y=ypts;
z=zpts;
title('triangular model of the scattering surface')
xlabel('x')
ylabel('y')
zlabel('z')
for i=1:nvert
    text(x(i)-max(x)/20,y(i)-max(x)/20,z(i),num2str(i))
end
hold off
disp('hit return to continue calculation')
pause
% label
% Define position vectors to vertices
for i=1:nvert;
    r(i,:)=[x(i) y(i) z(i)];
end
% Get edge vectors and normals from edge cross products
for i=1:ntria
    A=r(vind(i,2),:)-r(vind(i,1),:);
    B=r(vind(i,3),:)-r(vind(i,1),:);
    C=r(vind(i,3),:)-r(vind(i,2),:);
    N(i,:)=cross(A,B);
% check for proper direction of normal vector
if N(i,3)<0
    N(i,:)=-N(i,:);
end
% Edge lengths for triangle "i"
    d(i,1)=norm(A);
    d(i,2)=norm(B);

```

```

        d(i,3)=norm(C);
        ss=.5*sum(d(i,:));
        Area(i)=sqrt(ss*(ss-d(i,1))*(ss-d(i,2))*(ss-d(i,3)));
        Nn=norm(N(i,:));
        N(i,:)=N(i,:)/Nn;
%transform triangles into local coordinates
x1=[1 0 0];
y1=[0 1 0];
z1=[0 0 1];
end
% Pattern Loop
it=0;
k=0;
load du.m;
for u1=-1:du:1-du
    for v1=-1:du:1-du;
        it=it+1;
%test to see if center of box is within visible region
        test=((u1+du/2)^2+(v1+du/2)^2);
        if test<=1
            k=k+1;
            phi=atan2((v1+du/2),(u1+du/2));
            cp=cos(phi); sp=sin(phi);
            theta=asin(sqrt(test));
            st=sin(theta); ct=cos(theta);
% Center of box is used so u and v are redefined using center
of % box
            u(k)=st*cp; v(k)=st*sp; w=ct;
            up=ct*cp; vp=ct*sp; wp=-st;
% Spherical coordinate system unit vectors

```

```

        R(it,:)= [u(k) v(k) w];
% Change Efield into global rectangular coordinates
strtra(1,:)= [st*cp ct*cp -sp];
strtra(2,:)= [st*sp ct*sp cp];
strtra(3,:)= [ct -st 0];
sei=[0 Et Ep];
ei=strtra*sei';
% Begin loop over triangles
        sumt=0;
        sump=0;
for m=1:ntria
t(m,:)=cross(z1,N(m,:));
beta(m)=acos(N(m,3));
alpha(m)=atan2(t(m,2),t(m,1)+1e-6)-pi/2;
% Test to see if front face is illuminated
        ndotk=N(m,:)*R(it,:);
        if ndotk >= 0 & iflag==0 | iflag~=0
%translation into local coordinates
%first rotate about z axis
tra1(1,:)= [cos(alpha(m)) sin(alpha(m)) 0];
tra1(2,:)= [-sin(alpha(m)) cos(alpha(m)) 0];
tra1(3,:)= [0 0 1];
% Rotation about yp axis
tra2(1,:)= [cos(beta(m)) 0 -sin(beta(m))];
tra2(2,:)= [0 1 0];
tra2(3,:)= [sin(beta(m)) 0 cos(beta(m))];
D1=tra1*R(it,:);
D2=tra2*D1;
upp=D2(1);
vpp=D2(2);

```

```

wpp=D2(3);
% Find spherical angles in local coordinates
stpp=sqrt(upp^2+vpp^2)*sign(wpp);
ctpp=sqrt(1-stpp^2);
thpp=acos(ctpp);
phipp=atan2(vpp,upp+1e-10);
% Phase at the three vertices of triangle m; monostatic RCS
needs % "2"
    Dp=2*bk*((x(vind(m,1))-x(vind(m,3)))*u(k)+...

(y(vind(m,1))-y(vind(m,3)))*v(k)+...

(z(vind(m,1))-z(vind(m,3)))*w);
    Dq=2*bk*((x(vind(m,2))-x(vind(m,3)))*u(k)+...

(y(vind(m,2))-y(vind(m,3)))*v(k)+...

(z(vind(m,2))-z(vind(m,3)))*w);

Do=2*bk*(x(vind(m,3))*u(k)+y(vind(m,3))*v(k)+z(vind(m,3))*w);

%incident field in local rectangular coordinates
eip=tral*ei;
eipp=tra2*eip;
% translation of E-field into local spherical coordinates
strtra2=[stpp*cos(phipp)    ctp*cos(phipp)    -sin(phipp);
stpp*sin(phipp) ctp*sin(phipp) cos(phipp); ctp -stpp 0];
epp=strtra2^(-1)*eipp;
% Area integral for general case
DD=Dq-Dp;

```

```

expDo=exp(j*Do);
expDp=exp(j*Dp);
expDq=exp(j*Dq);
% Special Case 1
if abs(Dp) < Lt & abs(Dq) >= Lt
    sic=0.;
    for n=0:Nt

sic=sic+(j*Dp)^n/fact(n)*(-Co/(n+1)+expDq*(Co*gf(n,-Dq)));
        end
        Ic(k,m)=sic*2*Area(m)*expDo/j/Dq;
% Special Case 2
        elseif abs(Dp) < Lt & abs(Dq) < Lt
            sic=0.;
            for n=0:Nt

                                                for nn=0:Nt

sic=sic+(j*Dp)^n*(j*Dq)^nn/fact(nn+n+2)*Co;
                                                end

            end
            Ic(k,m)=sic*2*Area(m)*expDo;
% Special Case 3
            elseif abs(Dp) >= Lt & abs(Dq) < Lt
                sic=0.;
                for n=0:Nt

sic=sic+(j*Dq)^n/fact(n)*Co*gf(n+1,-Dp)/(n+1);
                    end
                    Ic(k,m)=sic*2*Area(m)*expDo*expDp;
% Special Case 4

```

```

elseif abs(Dp) >= Lt & abs(Dq) >= Lt & abs(DD) < Lt
    sic=0.;
    for n=0:Nt
        sic = sic+(j*DD)^n/fact(n)*(-Co*gf(n,Dq)+expDq*Co/(n+1));
    end
    Ic(k,m)=sic*2*Area(m)*expDo/j/Dq;
else
    Ic(k,m)=2*Area(m)*expDo*(expDp*Co/Dp/DD-expDq*Co/Dq/DD-Co/Dp
/Dq);
end
% end of special cases test
end %end of illumination test
end %end of triangle loop
Eth2(k)=Eth(it);
end % end of test for visible region
end % end of v loop
end % end of u loop
ac=pinv(Ic)*Eth2';
for k=1:ntria
    if imag(ac(k))<=.0001
        ac(k)=real(ac(k));
    end
    sr(k)=(1/ac(k)-1)*.5;
    % correct round-off
    s(k)=round(sr(k)*1e4);
    sr(k)=s(k)*1e-4;
end
k=1:ntria;
figure(2)
plot(k,rs,k,sr,'-');

```

```
title('Comparison of Original and Synthesized Resistivity')  
xlabel('Triangle Number')  
ylabel('Normalized Resistivity')
```

```

% POTES.M
% PO scattering from triangles
clear all
% illumination flag: =0 external face only
iflag=1;
Lt=.001;
Nt=2;
wave=1;
bk=2*pi/wave;
rad=pi/180;
% Incident wave polarization
Et=1+j*0; %TM-z
Ep=0+j*0; %TE-z
phi=0;
phr=phi*rad;
cp=cos(phr);sp=sin(phr);
% Wave amplitude at all vertices
Co=1.;
build
ntria=nfaces;
nvert=nverts;
x=xpts;
y=ypts;
z=zpts;
title('triangular model of the scattering surface')
xlabel('x')
ylabel('y')
zlabel('z')
for i=1:nvert
    text(x(i)-max(x)/20,y(i)-max(x)/20,z(i),num2str(i))

```

```

end
hold off
disp('hit return to continue calculation')
pause

% Define position vectors to vertices
for i=1:nvert;
    r(i,:)=[x(i) y(i) z(i)];
end
%Use synthesized resistivity
%load sr0.m                % 0 resistivity
%load srl.m                % 377 ohm/sq resistivity
load srl.m                 % linear resistivity
rs=srl;
% edge vectors and normals from edge cross products
for i=1:ntria
    A=r(vind(i,2),:)-r(vind(i,1),:);
    B=r(vind(i,3),:)-r(vind(i,1),:);
    C=r(vind(i,3),:)-r(vind(i,2),:);
    N(i,:)=cross(A,B);

% check for proper direction of normal vector
if N(i,3)<0
    N(i,:)=-N(i,:);
end

% Edge lengths for triangle "i"

    d(i,1)=norm(A);

```

```

    d(i,2)=norm(B);
    d(i,3)=norm(C);
    ss=.5*sum(d(i,:));
    Area(i)=sqrt(ss*(ss-d(i,1))*(ss-d(i,2))*(ss-d(i,3)));
    Nn=norm(N(i,:));
    N(i,:)=N(i,:)/Nn;

%transform triangles into local coordinates
x1=[1 0 0];
y1=[0 1 0];
z1=[0 0 1];
end
% Pattern Loop
start=0;
stop=180;
del=1;
it=floor((stop-start)/del)+1;
for i=1:it
    theta(i)=start+(i-1)*del;
    thr=theta(i)*rad;
    st=sin(thr); ct=cos(thr);
    u=st*cp; v=st*sp; w=ct;
    up=ct*cp; vp=ct*sp; wp=-st;
% Spherical coordinate system unit vectors
    R(i,:)=[u v w];
% Change Efield into global rectangular coordinates
    strtra(1,:)=[st*cp ct*cp -sp];
    strtra(2,:)=[st*sp ct*sp cp];
    strtra(3,:)=[ct -st 0];
    sei=[0 Et Ep];

```

```

ei=strtra*sei';
% correct orientation for normal after 90deg
if theta(i)==91
    N=-N;
end
% Begin loop over triangles
    sumt=0;
    sump=0;
for m=1:ntria
    t(m,:)=cross(z1,N(m,:));
    beta(m)=acos(N(m,3));
    alpha(m)=atan2(t(m,2),t(m,1)+1e-6)-pi/2;
    % Test to see if front face is illuminated
        ndotk=N(m,:)*R(i,:)';
        if ndotk >= 0 & iflag==0 | iflag~=0
%translation into local coordinates
%first rotate about z axis
tral(1,:)=[cos(alpha(m)) sin(alpha(m)) 0];
tral(2,:)=[-sin(alpha(m)) cos(alpha(m)) 0];
tral(3,:)=[0 0 1];
% Rotation about yp axis
tra2(1,:)=[cos(beta(m)) 0 -sin(beta(m))];
tra2(2,:)=[0 1 0];
tra2(3,:)=[ sin(beta(m)) 0 cos(beta(m))];
D1=tral*R(i,:)';
D2=tra2*D1;
upp=D2(1);
vpp=D2(2);
wpp=D2(3);
% Find spherical angles in local coordinates

```

```

stpp=sqrt(upp^2+vpp^2)*sign(wpp);
ctpp=sqrt(1-stpp^2);
thpp=acos(ctpp);
phipp=atan2(vpp,upp+1e-10);
% Phase at the three vertices of triangle m; monostatic RCS
needs % "2"
    Dp=2*bk*((x(vind(m,1))-x(vind(m,3)))*u+...

(y(vind(m,1))-y(vind(m,3)))*v+...

(z(vind(m,1))-z(vind(m,3)))*w);
    Dq=2*bk*((x(vind(m,2))-x(vind(m,3)))*u+...

(y(vind(m,2))-y(vind(m,3)))*v+...

(z(vind(m,2))-z(vind(m,3)))*w);
    Do=2*bk*(x(vind(m,3))*u+y(vind(m,3))*v+z(vind(m,3))*w);
%incident field in local rectangular coordinates
eip=tra1*ei;
eipp=tra2*eip;
% translation of E-field into local spherical coordinates
strtra2=[stpp*cos(phipp)    ctp*cos(phipp)    -sin(phipp);
stpp*sin(phipp) ctp*sin(phipp) cos(phipp); ctp -stpp 0];
epp=strtra2^(-1)*eipp;
%Reflection coefficients
gamp=0;
    if (2*rs(m)+ctpp)~=0
        gamp=1/(2*rs(m)+ctpp);
    end
gamn=1/(2*rs(m)*cos(thpp)+1);

```

```

%Surface Currents
Jxpp(i,m)=(epp(2)*gamp-epp(3)*gamn)*ctpp^2;
Jypp(i,m)=(epp(2)*gamp+epp(3)*gamn)*ctpp;
% Area integral for general case
DD=Dq-Dp;
expDo=exp(j*Do);
expDp=exp(j*Dp);
expDq=exp(j*Dq);
% Special Case 1
if abs(Dp) < Lt & abs(Dq) >= Lt
%disp('case 1')
    icafe(i,m)=1;
    sic=0.;
    for n=0:Nt

sic=sic+(j*Dp)^n/fact(n)*(-Co/(n+1)+expDq*(Co*gf(n,-Dq)));
    end
    Ic(i,m)=sic*2*Area(m)*expDo/j/Dq;
% Special Case 2
    elseif abs(Dp) < Lt & abs(Dq) < Lt
%disp('case 2')
    icafe(i,m)=2;
    sic=0.;
    for n=0:Nt

                                for nn=0:Nt

sic=sic+(j*Dp)^n*(j*Dq)^nn/fact(nn+n+2)*Co;
    end
    end
    Ic(i,m)=sic*2*Area(m)*expDo;

```

```

% Special Case 3
    elseif abs(Dp) >= Lt & abs(Dq) < Lt
%disp('case 3')
        icafe(i,m)=3;
        sic=0.;
        for n=0:Nt

sic=sic+(j*Dq)^n/fact(n)*Co*gf(n+1,-Dp)/(n+1);
            end
            Ic(i,m)=sic*2*Area(m)*expDo*expDp;
% Special Case 4
        elseif abs(Dp) >= Lt & abs(Dq) >= Lt & abs(DD) < Lt
%disp('case 4')
            icafe(i,m)=4;
            sic=0.;
            for n=0:Nt
                sic = sic+(j*DD)^n/fact(n)*(-Co*gf(n,Dq)+expDq*Co/(n+1));
            end
            Ic(i,m)=sic*2*Area(m)*expDo/j/Dq;
            else
                icafe(i,m)=0;
Ic(i,m)=2*Area(m)*expDo*(expDp*Co/Dp/DD-expDq*Co/Dq/DD-Co/Dp
/Dq);
            end
% end of special cases test
%Scattered field in local rectangular coordinates
Esxpp=Jxpp(i,m)*Ic(i,m);
Esypp=Jypp(i,m)*Ic(i,m);
Eszpp=0;
%retranslation to global rectangular coordinates

```

```

Espp(m,:)=[Esxpp Esypp Eszpp];
Es1=tra2^(-1)*Espp(m,:);
Es=tra1^(-1)*Es1;
%retranslation to global spherical coordinates
%seipp(m,:)=strtra^(-1)*Es;
seipp(m,1)=0;
seipp(m,2)=ct*cp*Es(1)+ct*sp*Es(2)-st*Es(3);
seipp(m,3)=-sp*Es(1)+cp*Es(2);
%sum over all triangles to get scattered field
sumt=sumt+seipp(m,2);
sump=sump+seipp(m,3);
end %end of illumination test
end %end of triangle loop
Eth=sumt;
Sth(i)=10*log10(4*pi*abs(Eth)^2+1.e-10);
Eph=sump;
Sph(i)=10*log10(4*pi*abs(Eph)^2+1.e-10);
end
Sth(:)=max(Sth(:),-50);
Sph(:)=max(Sph(:),-50);
%load rcs0.m
%load rcs1.m
load rcs1.m
%plot rcs
figure(2)
plot(theta,rcs1,theta,Sth,'--'),grid
title('solid:original    dashed:synthesized')
xlabel('monostatic angle, theta (deg)')
ylabel('sigma/wav1^2 (dB)')

```



## LIST OF REFERENCES

1. Price, Alfred, *The History of US Electronic Warfare Vol II*, The Association of Old Crows, 1989.
2. Knott, E. F., Shaeffer, J. F. and Tuley, M. T., *Radar Cross Section*, Artech House, Norwood, MA, 1993.
3. Jenn, D. C., *Radar and Laser Cross Section Engineering*, American Institute of Aeronautics and Astronautics, Inc., New York, NY, 1995.
4. Balanis, C. A., *Advanced Engineering Electromagnetics*, John Wiley & Sons, New York, NY, 1989.
5. Faros, N. I., "Radar Cross Section Synthesis for Planar Resistive Surfaes," Master's thesis, Naval Postgraduate School, 1994.
6. Moreira, F. J. S. and Prata, A., "A Self-Checking Predictor-Corrector Algorithm for Efficient Evaluation of Reflector Antenna Radiation Integrals," *IEEE Trans. on Antennas and Propagation*, Vol. 42, No. 2, pp. 246-254, 1994.



## INITIAL DISTRIBUTION LIST

	No. Copies
1. Defense Technical Information Center Cameron Station Alexandria, Virginia 22304-6145	2
2. Library, Code 013 Naval Postgraduate School Monterey, California 93943-5101	2
3. Chairman, Code EC Department of Electrical and Computer Engineering Naval Postgraduate School Monterey, California 93943-5121	1
4. Professor David C. Jenn, Code EC/Jn Department of Electrical and Computer Engineering Naval Postgraduate School Monterey, California 93943-5121	2
5. Professor Hung-Mou Lee, Code EC/Lh Department of Electrical and Computer Engineering Naval Postgraduate School Monterey, California 93943-5121	1
6. Rachel C. Waddell Route One Box 102B Westville, Florida 32464	2